

Supporting Information

Apoptosis-Inducing Activity of a Fluorescent Barrel-Rosette M^+/Cl^- Channel

Javid Ahmad Malla,^a Rintu M. Umesh,^b Amal Vijay,^a Arnab Mukherjee,^a Mayurika Lahiri,^b and Pinaki Talukdar^{*a}

^a Department of Chemistry, Indian Institute of Science Education and Research Pune, Dr. Homi Bhabha Road, Pashan, Pune 411008, Maharashtra (India)

^b Department of Biology, Indian Institute of Science Education and Research Pune, Dr. Homi Bhabha Road, Pashan, Pune 411008, Maharashtra (India)

Table of Contents

No.	Contents	Page Number
I	General Methods	S2
II	Physical Measurements	S2 – S3
III	Estimation of pK_a and $\log P$ Values	S3
IV	Synthesis	S3 – S5
V	Ion Transport Studies	S5 – S14
VI	Planar Bilayer Conductance Studies	S15 – S16
VII	Ion transport in DPPC Vesicles	S16 – S17
VIII	Single Crystal X-Ray Diffraction Study	S17 – S18
IX	Theoretical Calculations	S18 – S23
X	UV-Visible Spectral Studies	S23 – S24
XI	Biological Studies	S24 – S29
XII	NMR Spectra	S30 – S39
XII	References	S40– S41

I. General Methods:

All reactions were carried out under the nitrogen atmosphere. All the chemicals were purchased from commercial sources and were used as received unless stated otherwise. Solvents were dried by standard methods prior to use or purchased as dry. Thin layer chromatography (TLC) was carried out with E. Merck silica gel 60-F₂₅₄ plates and column chromatography was performed over silica gel (100-200 mesh) obtained from commercial suppliers. Egg yolk phosphatidylcholine (EYPC) lipid was purchased from Avanti Polar Lipids as a solution dissolved in chloroform (25 mg/mL). HEPES buffer, HPTS dye, Carboxyfluorescein (CF) system, Triton X-100, NaOH and all inorganic salts of molecular biology grade were purchased from Sigma. Gel-permeation chromatography was performed on a column of Sephadex LH-20 gel (25 × 300 mm, V₀ = 25 mL). Large unilamellar vesicles (LUV) were prepared from EYPC lipid by using mini extruder, equipped with a polycarbonate membrane either of 100 nm or 200 nm pore size, obtained from Avanti Polar Lipids.

II. Physical Measurements:

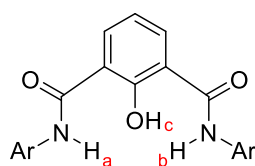
The ¹H and ¹³C NMR spectra were recorded on 400 MHz Jeol ECS-400 (or 100 MHz for ¹³C) spectrometers using either residual solvent signals as an internal reference or from internal tetramethylsilane on the δ scale relative to chloroform (δ 7.26), dimethylsulphoxide (δ 2.50 ppm), acetone (δ 2.05) for ¹H NMR and chloroform (δ 77.20 ppm), dimethylsulphoxide (δ 39.50 ppm), acetone (δ 29.84 and 206.26) for ¹³C NMR. The chemical shifts (δ) are reported in ppm and coupling constants (J) in Hz. The following abbreviations are used: s (singlet), d (doublet) m (multiplet), and td (triplet of doublet) while describing ¹H NMR signals. High-resolution mass spectra (HRMS) were obtained from MicroMass ESI-TOF MS spectrometer. All the FT-IR spectra were taken and reported in wave numbers (cm⁻¹) using a solution of compound in 30% MeOH/CHCl₃. Fluorescence spectra were recorded by using Fluoromax-4 from Jobin Yvon Edison equipped with an injector port and a magnetic stirrer. 10 mM HEPES (with 100 mM NaCl or other salts as per necessity) buffer solutions were used for fluorescence experiment and the pH of the buffers were adjusted to 7.0 or 8.0 by NaOH and pH of the buffer solutions was measured using Helmer pH meter. Melting points of all the compounds were measured using a

VEEGO Melting point apparatus. All melting points were measured in open glass capillary and values are uncorrected. All fluorescence data were processed either by Origin 8.5 or KaleidaGraph and finally, all data were processed through ChemDraw Professional 15.

III. Estimation of pK_a and $\log P$ Values:

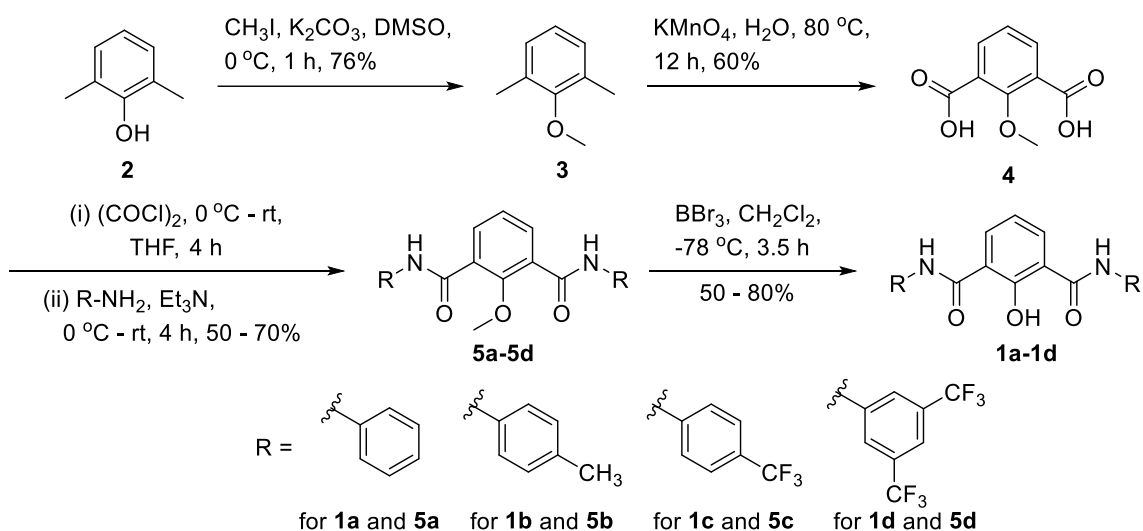
The calculator plugins of MarvinSketch program was used to estimate the pK_a and $\log P$ values of compounds **1a–1d**.^{S1}

Table S1. Estimated pK_a and $\log P$ values of compounds **1a–1d**.



Compound	pK_a value			$\log P$
	For proton a	For proton b	For proton c	
1a	12.77	12.00	6.42	3.85
1b	12.95	12.17	6.42	4.88
1c	12.41	11.63	6.42	5.61
1d	11.27	10.50	6.42	7.36

IV. Synthesis



Scheme S1. Synthesis of compounds **1a–1d**.

Synthesis of compound 3: Synthesis of compound **2** was done according to the known protocol.^{S2}

Synthesis of compound 4: Synthesis of compound **3** was also done according to the known protocol.^{S3}

General method for synthesis of 1a–1d.

The compound **4** converted to corresponding acid chloride by using oxalyl chloride at 0 °C for four hours. Then, the respective amine was added at 0 °C and the reaction mixture was allowed to come to room temperature and stirred for four hours to get **5a–5d**. The compound so formed was directly treated with boron tribromide in CH₂Cl₂ (1 M BBr₃ in CH₂Cl₂) at -78 °C. The reaction mixture was allowed to come to room temperature and stirred for three hours. Then, the reaction mixture was washed with sodium bicarbonate and organic layer was collected in dichloromethane and dried using sodium sulfate and solvent was removed *in vacuo*. The purification was done using silica gel chromatography to get the desired compounds **1a–1d** with 50% to 80% yields.

Compound 1a: Pale yellow solid (75% yield); **M.p.:** 183.0–185.0 °C; **IR** (v/cm⁻¹) 3322, 3062, 2929, 2832, 1652, 1594, 1535, 1485, 1337, 1151, 748; **¹H NMR (400 MHz, CDCl₃)** δ 14.35 (s, 1H), 9.30 (t, 2H), 8.14 (d, *J* = 7.8 Hz, 2H), 7.69 (d, *J* = 8.7 Hz, 4H), 7.42 (t, *J* = 7.9 Hz, 4H), 7.22 (t, *J* = 7.9 Hz, 2H), 7.08 (t, *J* = 7.8 Hz, 1H); **¹³C NMR (100 MHz, CDCl₃)**: δ 165.92, 160.30, 137.19, 133.58, 129.11, 125.19, 121.33, 119.05, 118.48; **HRMS (ESI):** Calc. for C₂₀H₁₆N₂O₃ [M+H]⁺: 333.1239; Found: 333.1278.

Compound 1b: White solid (65% yield); **M.p.:** 204.0–206.0 °C; **IR** (v/cm⁻¹) 3342, 2951, 2839, 1651, 1605, 1437, 1352, 1112, 1017, 751; **¹H NMR (400 MHz, CDCl₃)**: δ 9.20 (s, 2H), 8.08 (d, *J* = 7.8 Hz, 2H), 7.52 (d, *J* = 8.4 Hz, 4H), 7.18 (dd, *J* = 8.0 Hz, 4H), 7.02 (t, *J* = 7.9 Hz, 1H), 2.34 (s, 6H); **¹³C NMR (100 MHz, CDCl₃)**: δ 165.60, 160.28, 134.90, 134.58, 133.31, 129.64, 121.14, 119.07, 20.97; **HRMS (ESI):** Calc. for C₂₂H₂₀N₂O₃ [M+H]⁺: 361.1552; Found: 361.1578.

Compound 1c: White solid (58% yield); **M.p.:** 213.0–215.0 °C; **IR** (v/cm^{-1}) 3310, 2947, 2835, 1657, 1547, 1414, 1326, 1101, 1018, 753; **^1H NMR (400 MHz, DMSO):** δ 10.95 (s, 2H), 8.11 (d, $J = 7.8$ Hz, 2H), 7.98 (d, $J = 8.5$ Hz, 4H), 7.77 (d, $J = 8.7$ Hz, 4H), 7.14 (t, $J = 7.7$ Hz, 1H) **^{13}C NMR (100 MHz, DMSO):** δ 167.08 (s), 142.35 (s), 133.52 (s), 126.52 (q, $J = 7.4, 3.6$ Hz), 126.13 (s), 124.61 (d, $J = 31.8$ Hz), 123.44 (s), 121.06 (d, $J = 10.5$ Hz), 120.63 (s).; **^{19}F NMR (377 MHz, DMSO):** δ -60.44 (s); **HRMS (ESI):** Calc. for $\text{C}_{22}\text{H}_{14}\text{F}_6\text{N}_2\text{O}_3$ $[\text{M}+\text{H}]^+$: 469.0987; Found: 469.0987.)

Compound 1d: White solid (50% yield); **M.p.:** 217.0–219.0 °C; **IR** (v/cm^{-1}) 3344, 2942, 2832, 1658, 1550, 1454, 1220, 1115, 1022, 749; **^1H NMR (400 MHz, $\text{CD}_3\text{OD}:\text{CDCl}_3$):** δ 14.10 (s, 1H), 9.57 (s, 2H), 8.22 (s, 6H), 7.72 (s, 2H), 7.19 (t, $J = 7.9$ Hz, 1H). **^{13}C NMR (100 MHz, $\text{CD}_3\text{OD}:\text{CDCl}_3$):** δ 170.70 (s), 143.24 (s), 138.43 (s), 136.11 (q, $J = 33.4$ Hz), 131.13 (s), 128.42 (s), 125.71 (s), 124.76 (s), 123.14 (d, $J = 28.6$ Hz), 121.71 (q, $J = 13.6, 10.1$ Hz); **^{19}F NMR (377 MHz, CDCl_3):** δ -63.02 (s); **HRMS (ESI):** Calc. for $\text{C}_{24}\text{H}_{12}\text{F}_{12}\text{N}_2\text{O}_3$ $[\text{M}+\text{H}]^+$: 605.0735; Found: 605.0743.

V. Ion Transport Studies:

Buffer and stock solution preparation: HEPES buffer (10 mM) was prepared by dissolving solid HEPES in autoclaved water, then NaCl (100 mM) was added and followed by adjustment of pH = 7.0 by adding NaOH solution. Stock solutions of all compounds were prepared in either HPLC grade DMSO (for HPTS assay) and in 1:1 MeOH/THF (for Lucigenin assay).

Preparation of EYPC-LUVs Δ HPTS: Vesicles were prepared according to the reported protocol.^{4,5}

Ion transport activity: 1975 μL of HEPES buffer (10 mM HEPES, 100 mM NaCl, pH = 7.0) was taken in a clean fluorescence cuvette followed by addition of 25 μL of EYPC-LUVs Δ HPTS in the same cuvette and was placed on the fluorescence instrument (at $t = 0$ s) equipped with magnetic stirrer. Fluorescence emission intensity of HPTS dye, F_t was monitored at $\lambda_{\text{em}} = 510$ nm ($\lambda_{\text{ex}} = 450$ nm) with time. After that, a pH gradient between the intra and extra vesicular system was created by adding 20 μL of 0.5 M NaOH to the same cuvette at $t = 20$ s (Figure S1). All compounds were added at $t = 100$ s in different concentrations and finally, at $t = 300$ s, 25 μL

of 10% Triton X-100 was added to destroy all vesicles which resulted in the destruction of pH gradient (Figure. S2), which resulted in saturation in fluorescence emission intensity.

The time axis was normalized according to Equation S1:

$$t = t - 100 \quad \text{(Equation S1)}$$

The time of compound addition can be normalized to $t = 0$ s and time of Triton-X 100 addition was normalized to $t = 200$ s.

Fluorescence intensities (F_t) were normalized to fractional emission intensity I_F using Equation S2:

$$I_F = [(F_t - F_0)/(F_\infty - F_0)] \times 100 \quad \text{(Equation S2)}$$

where, F_0 = Fluorescence intensity just before the compound addition (at $t = 0$ s). F_∞ = Fluorescence intensity at saturation after complete leakage (at $t = 340$ s). F_t = Fluorescence intensity at time t .

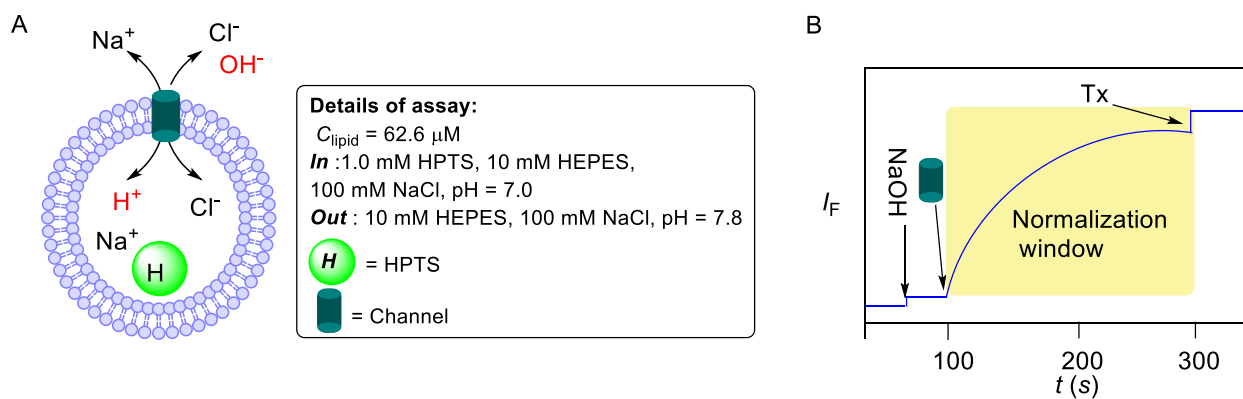


Fig. S1 Schematic illustration of ion transport activity assay using EYPC-LUVs with HPTS (**A**) and representative fluorescence kinetics experiment of ion transport (**B**).

Ion transport kinetics was studied at different concentrations for each compound. Change of HPTS emission intensity in this process was monitored with time.

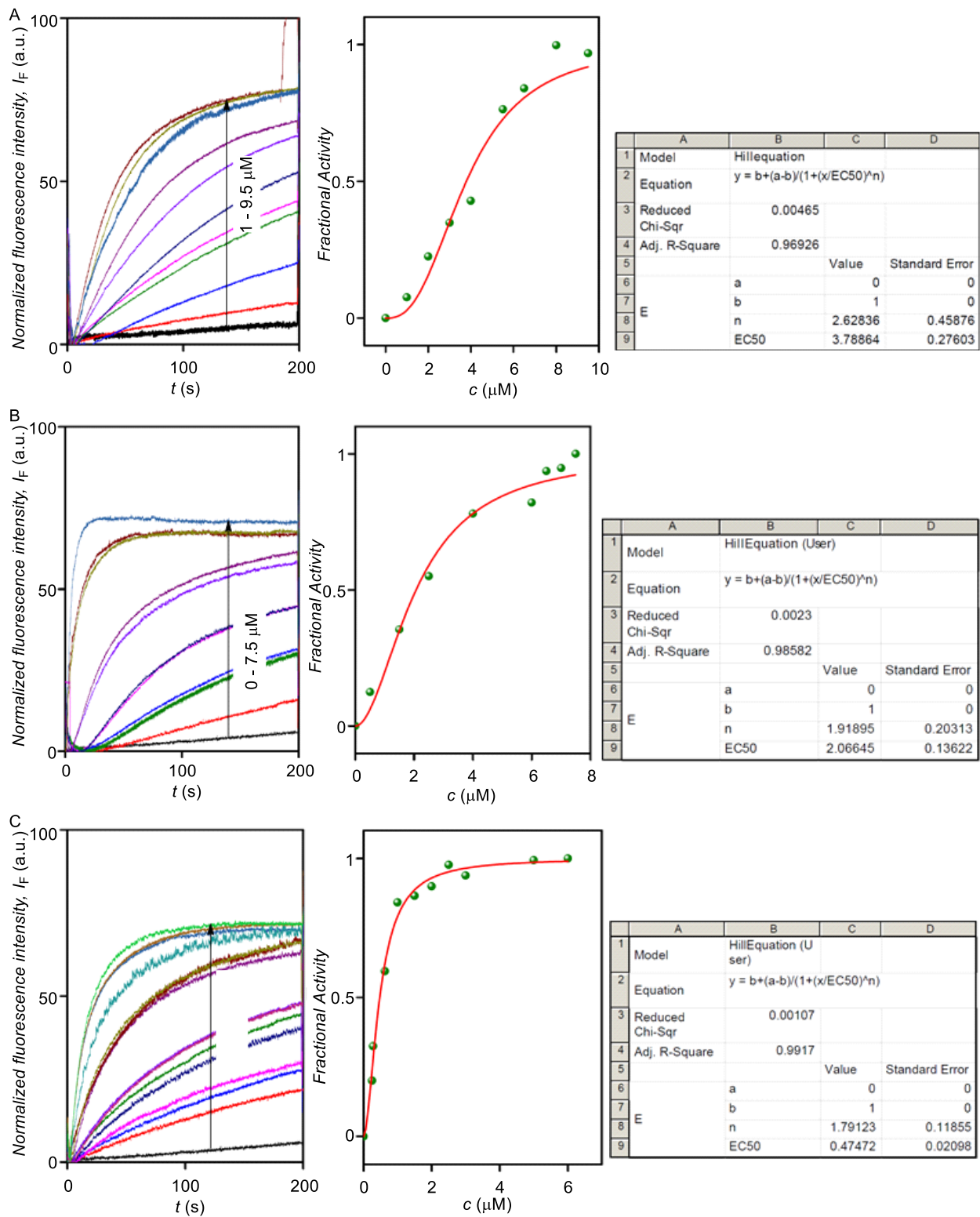


Fig. S2 Dose-response curves and Hill analysis of compound **1b** (A), **1c** (B), and **1d** (C).

The concentration profile data were analyzed by Hill Equation (Equation S3) to get the Effective concentration (EC_{50}) and Hill coefficient (n), (Figure S3).

$$Y = Y_{\infty} + (Y_0 - Y_{\infty}) / [1 + (c / EC_{50})^n] \quad \text{(Equation S3)}$$

where, Y_0 = Fluorescence intensity just before the channel addition (at $t = 0$ s). Y_{∞} = Fluorescence intensity with excess channel concentration, c = Concentration of channel forming molecule.

Determination of Ion Selectivity by HPTS assay:^{S6}

Buffer and Stock Solution Preparation: HEPES buffers with all salts were prepared by dissolving solid HEPES (10 mM) followed by addition of appropriate salt (100 mM) in autoclaved water and adjustment of pH (pH = 7.0) was done by dropwise addition of NaOH solution.

Preparation of EYPC-LUVs \Rightarrow HPTS for Cation Selectivity: EYPC-LUVs \Rightarrow HPTS (~ 5.0 mM EYPC, inside: 1 mM HPTS, 10 mM HEPES, 100 mM NaCl, pH = 7.0 and outside: 10 mM HEPES, 100 mM NaCl, pH = 7.0) were prepared following reported protocol.^[S3-S5]

Cation Selectivity Assay: In a clean fluorescence cuvette 1975 μ L of different HEPES buffer solutions (10 mM HEPES, 100 mM MCl, pH = 7.0; where, M^+ = Li^+ , Na^+ , K^+ , Rb^+ and Cs^+)^{S10} were taken followed by addition of 25 μ L of EYPC-LUVs \Rightarrow HPTS vesicle in slowly stirring condition by a magnetic stirrer equipped with the fluorescence instrument (at $t = 0$ s). The time course of HPTS fluorescence intensity, F_t was monitored at $\lambda_{em} = 510$ nm ($\lambda_{ex} = 450$ nm). At $t = 20$ s, 20 μ L of 0.5 M NaOH was added to the cuvette to make the pH gradient between the intra and extra vesicular system. The compound **1d** was added at $t = 100$ s and at $t = 300$ s, 10% Triton X-100 (25 μ L) was added to lyse all vesicles for the complete destruction of pH gradient. For data analysis and comparison, time (X-axis) was normalized between the point of channel addition (*i.e.* $t = 100$ s was normalized to $t = 0$ s) and end point of the experiment (*i.e.* $t = 300$ s was normalized to $t = 200$ s). Fluorescence intensities (F_t) were normalized to fractional emission intensity I_F using Equation S2.

Preparation of EYPC-LUVs Δ HPTS for Anion Selectivity:^{S6,7}

EYPC-LUVs Δ HPTS (~ 5.0 mM EYPC, inside: 1 mM HPTS, 10 mM HEPES, 100 mM NaX, pH = 7.0 and outside: 10 mM HEPES, 100 mM NaX, pH = 7.0; where, $X^- = Cl^-, Br^-, ClO_4^-, NO_3^-$ and I^-) were prepared following reported protocol.

Anion Selectivity Assay: In a clean fluorescence cuvette, 1975 μ L of HEPES buffer (10 mM HEPES, 100 mM NaX, at pH = 7.0; where, $X^- = Cl^-, Br^-, ClO_4^-, NO_3^-$ and I^- was added followed by addition of 25 μ L of EYPC-LUVs Δ HPTS vesicle in slowly stirring condition by a magnetic stirrer equipped with the fluorescence instrument (at $t = 0$ s). HPTS fluorescence emission intensity (F_t) was monitored with time at $\lambda_{em} = 510$ nm ($\lambda_{ex} = 450$ nm). 20 μ L of 0.5 M NaOH was added to the cuvette at $t = 20$ s to make the pH gradient between the intra and extra vesicular system. The compound **1d** was added at $t = 100$ s and at $t = 300$ s, 25 μ L of 10% Triton X-100 was added to lyse all vesicles for the complete destruction of pH gradient. For data analysis and comparison, time (X-axis) was normalized between the point of transporter addition (*i.e.* $t = 100$ s was normalized to $t = 0$ s) and end point of the experiment (*i.e.* $t = 300$ s was normalized to $t = 200$ s) using Equation S1. Fluorescence intensities (F_t) were normalized to fractional emission intensity I_F using Equation S2.

Determination of chloride ion influx by lucigenin assay:^{S8}

Preparation of EYPC-LUVs Δ Lucigenin for concentration dependent assay and symport assay: A solution (1 mL) of EYPC lipid (25 mg/mL) lipid dissolved in $CHCl_3$ was taken in a clean and dry small round bottom flask. The solvents were evaporated slowly by a stream of nitrogen, followed by drying under vacuum for at least 5 h. After that 1 mL of 1 mM *N,N'*-dimethyl-9,9'-biacridinium dinitrate (lucigenin) in 200 mM $NaNO_3$ (dissolved in 10 mM Hepes buffer with pH=7.0) was added, and the suspension was hydrated for 1 h with occasional vortexing of 4-5 times and then subjected to freeze-thaw cycle (≥ 15 times). The vesicle solution was extruded through a polycarbonate membrane with 200 nm pores for minimum 19 times (must be an odd number), to give vesicles with a mean diameter of ~ 200 nm. The extracellular lucigenin was removed from the vesicles by size exclusion column chromatography (Sephadex G-50) using 200 mM $NaNO_3$ as eluent. The obtained vesicles were diluted to 4 mL with 200 mM $NaNO_3$.

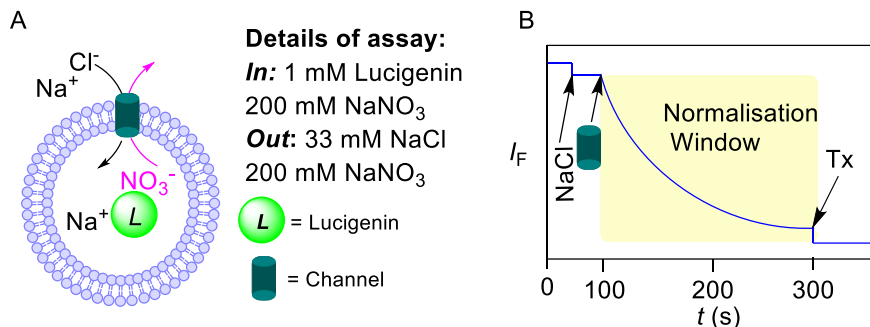


Fig. S3 Schematic illustration of chloride influx assay using EYPC-LUVs \supset Lucigenin (**A**) and representative fluorescence kinetics experiment of corresponding assay (**B**).

Chloride influx into EYPC-LUVs \supset Lucigenin: In a clean and dry fluorescence cuvette, 50 μ L of above lipid solution and 1950 μ L of 200 mM NaNO₃ solution was taken and kept in slowly stirring condition by a magnetic stirrer equipped with the fluorescence instrument (at $t = 0$ s). In this assay, the time course of lucigenin fluorescence emission intensity, F_t was observed at $\lambda_{em} = 535$ nm ($\lambda_{ex} = 450$ nm). 25 μ L of 2 N NaCl was added to the cuvette at $t = 50$ s to make the salt gradient between the intra and extra vesicular system. Compound **1d** was added at $t = 100$ s and finally at $t = 300$ s, 25 μ L of 10% Triton X-100 was added to lyse all vesicles for 100% chloride influx. Fluorescence intensities (F_t) were normalized to fractional emission intensity I_F using Equation S4.

$$\text{Normalized Fl Intensity } (I_F) = [(F_t - F_0) / (F_\infty - F_0)] \times (-100) \quad (\text{Equation S4})$$

Chloride influx into EYPC-LUVs \supset Lucigenin in the presence of valinomycin:

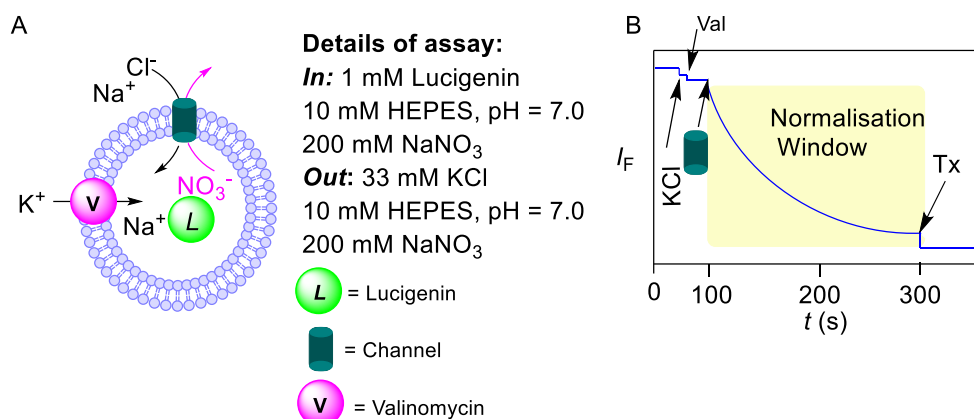


Fig. S4 Schematic illustration of chloride influx assay using EYPC-LUVs \supset Lucigenin in presence of valinomycin (A) and representative fluorescence kinetics experiment of corresponding assay (B).

Direct experimental insight of preferential transporting mechanism for **1d** was obtained by lucigenin assay in presence of valinomycin. Vesicles containing lucigenin and NaNO₃ were prepared and suspended in KCl solution and the ion transport rate of **1d** was monitored in absence and in presence of valinomycin. No significant difference in the rate of ion transport clearly proves symport mechanism is operating.

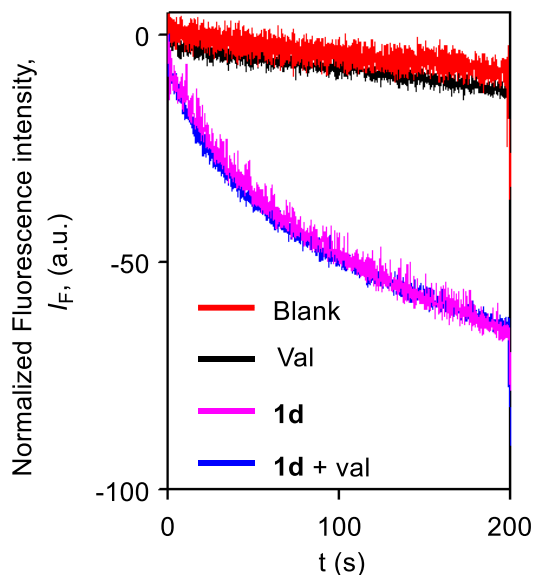


Fig. S5 Comparison of transport activity of **1d** (1.5 μ M) in the presence and absence valinomycin (0.125 μ M).

Effect of extravascular cations on the chloride influx into EYPC-LUVs \Rightarrow Lucigenin:

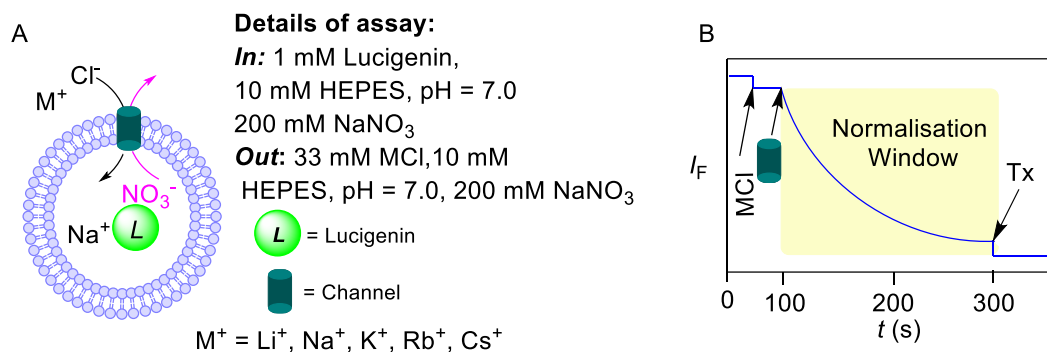


Fig. S6 Schematic illustration of chloride influx in presence of different metal cations using EYPC-LUVs \Rightarrow Lucigenin (**A**) and representative fluorescence kinetics experiment of corresponding assay (**B**).

In a clean and dry fluorescence cuvette, 50 μ L of above lipid solution and 1950 μ L of 200 mM NaNO₃ solution was taken and kept in slowly stirring condition by a magnetic stirrer equipped with the fluorescence instrument (at $t = 0$ s). In this assay, the time course of lucigenin fluorescence emission intensity, F_t was observed at $\lambda_{em} = 535$ nm ($\lambda_{ex} = 450$ nm). 25 μ L of 2 N MCl was added to the cuvette at $t = 50$ s to make the salt gradient between the intra and extra vesicular system. Compound **1d** was added at $t = 100$ s and finally at $t = 300$ s, 25 μ L of 10% Triton X-100 was added to lyse all vesicles for 100% chloride influx. Fluorescence intensities (F_t) were normalized to fractional emission intensity I_F using Equation S4.

Preparation of EYPC-LUVs \Rightarrow Lucigenin with intravesicular Cl⁻: A solution (1 mL) of EYPC lipid (25 mg/mL) dissolved in CHCl₃ was taken in a clean and dry small round bottom flask. The solvents were evaporated slowly by a stream of nitrogen, followed by drying under vacuum for at least 4 hours. After that 1 mL of 1 mM *N,N'*-dimethyl-9,9'-biacridinium dinitrate (lucigenin) in 200 mM NaCl (dissolved in 10 mM HEPES buffer with pH=7.0) was added, and the suspension was hydrated for 1 h with occasional vortexing of 4-5 times and then subjected to freeze-thaw cycle (≥ 15 times). The vesicle solution was extruded through a polycarbonate membrane with 200 nm pores 19 times (must be an odd number), to give vesicles with a mean diameter of ~ 200 nm. The extracellular lucigenin was removed from the vesicles by size exclusion column chromatography (Sephadex G-50) using 200 mM NaCl as eluent. The vesicles were diluted to 4 mL with 200 mM NaCl.

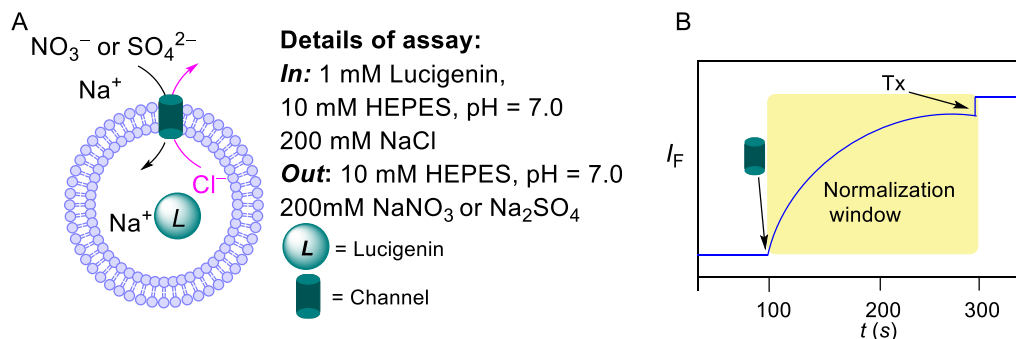


Fig. S7 Schematic illustration of chloride efflux assay using EYPC-LUVs \supset Lucigenin (**A**) and representative fluorescence kinetics experiment of corresponding assay (**B**).

Effect of extravesicular NO₃⁻ and SO₄²⁻ on the chloride efflux from EYPC-LUVs \supset Lucigenin: In a clean and dry fluorescence cuvette, 50 μ L of above lipid solution and 1950 μ L of an iso-osmolar solution of different NaX (X⁻ = NO₃⁻ and SO₄²⁻) salts were taken and kept in slowly stirring condition by a magnetic stirrer equipped with the fluorescence instrument (at t = 0 s). The time course of lucigenin fluorescence emission intensity, F_t was monitored at λ_{em} = 535 nm (λ_{ex} = 450 nm). Compound **1d** was added at t = 100 s and finally at t = 300 s, 25 μ L of 10% Triton X-100 was added to lyse all vesicles for 100% chloride efflux. Fluorescence intensities (F_t) were normalized to fractional emission intensity I_F using Equation S2.

Preparation of EYPC-LUVs \supset CF:^{S9} A thin lipid film was prepared by evaporating a solution of 12.5 mg EYPC in 0.5 ml CHCl₃ in vacuo for 4 h. After that lipid film was hydrated with 0.5 mL buffer (10 mM HEPES, 10 mM NaCl, 50 mM CF, pH 7.0) for 1 h with occasional vortexing of 4-5 times and then subjected to freeze-thaw cycle (\geq 20 times). The vesicle solution was extruded through a polycarbonate membrane with 100 nm pores 19 times (has to be an odd number), to give vesicles with a mean diameter of \sim 100 nm. The extracellular dye was removed size exclusion chromatography (Sephadex G-50) with 10 mM HEPES buffer (100 mM NaCl, pH 7.0. Final) Final concentration: \sim 2.5 mM EYPC lipid; intravesicular solution: 10 mM HEPES, 10 mM NaCl, 50 mM CF, pH 7.0; extravesicular solution: 10 mM HEPES, 100 mM NaCl, pH 7.0.

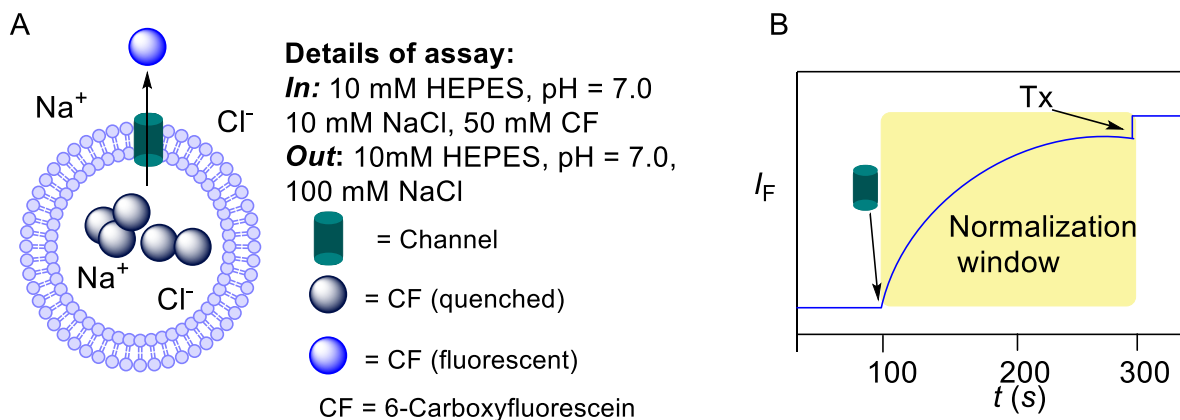


Fig. S8 Schematic illustration of CF leakage assay using EYPC-LUVs \Rightarrow HPTS, CF (A) and representative fluorescence kinetics experiment of corresponding assay (B).

CF leakage assay: In a clean and dry fluorescence cuvette 25 μ L of above lipid solution and 1975 μ L of 10 mM HEPES buffer (100 mM NaCl, pH 7.0) was taken and kept in slowly stirring condition by a magnetic stirrer equipped with the fluorescence instrument (at $t = 0$ s). The time course of CF fluorescence emission intensity, F_t was observed at $\lambda_{em} = 517$ nm ($\lambda_{ex} = 492$ nm). Compound **1d** was added at $t = 100$ s and finally at $t = 300$ s, 25 μ L of 10% Triton X-100 was added to lyse those vesicles for 100% chloride influx. Fluorescence intensities (F_t) were normalized to fractional emission intensity I_F according to Equation S2. This study confirmed that neither the bilayer membranes are defected nor large transmembrane pores are formed by **1d**.

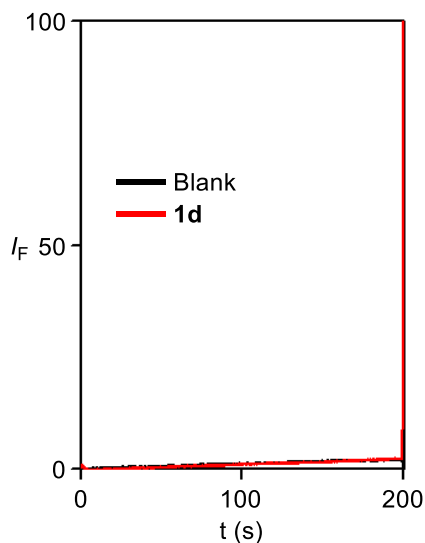


Fig. S9 Carboxyfluorescein efflux assay for compound **1d** (10 μ M).

VI. Planar Bilayer Conductance Measurements:^{S10}

Bilayer membrane (BLM) was formed across an aperture of 150 μM diameter in a polystyrene cup (Warner Instrument, USA) with lipid diphytanoylphosphatidylcholine (Avanti Polar Lipids), dissolved in *n*-decane (18 mg/mL). Both chambers (*cis* and *trans*) were filled with symmetrical solution, containing 1 M KCl. The *trans* compartment was held at virtual ground and the *cis* chamber was connected to the BC 535 head-stage (Warner Instrument, USA) via matched Ag-AgCl electrodes. Compound **1d** (2 μM) was added to the *trans* chamber and the solution was stirred with a magnetic stirrer for around 5 minutes. Channel formation was confirmed by the distinctive channel opening and closing events after applying voltages. Currents were low pass filtered at 1 kHz using pClamp9 software (Molecular Probes, USA) and an analog-to-digital converter (Digidata 1440, Molecular Probes). All data were analyzed by the software pClamp 9. The complete data trace observed for ten minutes contained a series of opening and closing events at some indefinite intervals. From a large and complete trace a small portion is presented in the manuscript (Figure 6A, B). The average current was calculated from this trace and then conductance and other calculations were made accordingly.

Calculation of ion channel diameter: Diameter of artificial ion channel was calculated according to Hille equation as given in the manuscript (equation 1).

Determination of anion selectivity permeability ratio by Planar Bilayer Conductance Measurements: The *cis* and *trans* chambers were filled with unsymmetric solutions of KCl. The *cis* chamber was filled with 1.0 M KCl solution and *trans* chamber was filled with 0.5 M KCl. The compound **1d** (2 μM) was added to the *trans* chamber and stirred for 5 minutes. The reversal potential was calculated to be 10 ± 2 mV (Fig. 6C).

The permeability ratio ($P_{\text{Cl}^-}/P_{\text{K}^+}$) was calculated by using Goldman-Hodgkin-Katz equation (Equation S5).

$$\frac{P_{\text{Cl}^-}}{P_{\text{K}^+}} = \frac{a_{\text{K}^+_{cis}} - a_{\text{K}^+_{trans}} \times \exp\left(-\frac{V_{\text{rev}} \times F}{R \times T}\right)}{a_{\text{Cl}^-_{cis}} \times \exp\left(-\frac{V_r \times F}{R \times T}\right) - a_{\text{Cl}^-_{trans}}} \quad (\text{S5})$$

where, $P_{\text{Cl}^-}/P_{\text{K}^+}$ = anion/cation permeability ratio; $a_{\text{K}^+_{cis}}$ = K^+ activity in the *cis* chamber; $a_{\text{K}^+_{trans}}$ = K^+ activity in the *trans* chamber; $a_{\text{Cl}^-_{cis}}$ = Cl^- activity in the *cis* chamber; $a_{\text{Cl}^-_{trans}}$ = Cl^- activity in the *trans* chamber; V_{rev} = reversal potential; F = Faraday constant; R = gas constant; T = temperature (K).

VII. Ion Transport using DPPC-LUVS \supset HPTS:^{S11}

Compound **1d** (1.5 μM in CH_3CN) was added to a solution of 1,2-dipalmitoyl-sn-glycero-3-phosphocholine (DPPC, 350 μL , 28.31 mM in deacidified CHCl_3). The receptor/lipid mixture was evaporated under a gentle stream of N_2 and dried under high vacuum for 1 hour. The resulting film was hydrated with 500 μL of an aqueous solution of HPTS dye (1 mM) in NaCl (100 mM) and was then sonicated for 30 seconds followed by stirring for 1 hour at 50 $^\circ\text{C}$ to give heterogenous LUVs. These heterogenous LUVs were disrupted by 10 freeze-thaw cycles and then the solution was carefully extruded (29 times) through a polycarbonate membrane (200 nm pore size) at 50 $^\circ\text{C}$ to give a uniform distribution of LUVs. The external HPTS was removed by passing the solution through a size exclusion column (sephadex 50G, eluted in 100 mM NaCl) and the collected vesicles were made up to a total volume of 2 mL (0.4 mM in lipid) with NaCl solution (100 mM). A cuvette containing 2 mL of the vesicle solution was placed in a fluorescence spectrometer and held at the temperature of interest (either 30 $^\circ\text{C}$ or 45 $^\circ\text{C}$). After the addition of NaOH (50 μL , 0.5 M) to the fluorescence decay was monitored over 280 seconds. The results are shown in Figure S8.

The time axis was normalized according to Equation S6:

$$t = t - 100 \quad \text{(Equation S6)}$$

The time of NaOH addition can be normalized to $t = 0$ s and time of Triton-X 100 addition was normalized to $t = 180$ s.

The fluorescence intensities (F_t) were normalized to fractional emission intensity I_F using Equation S2:

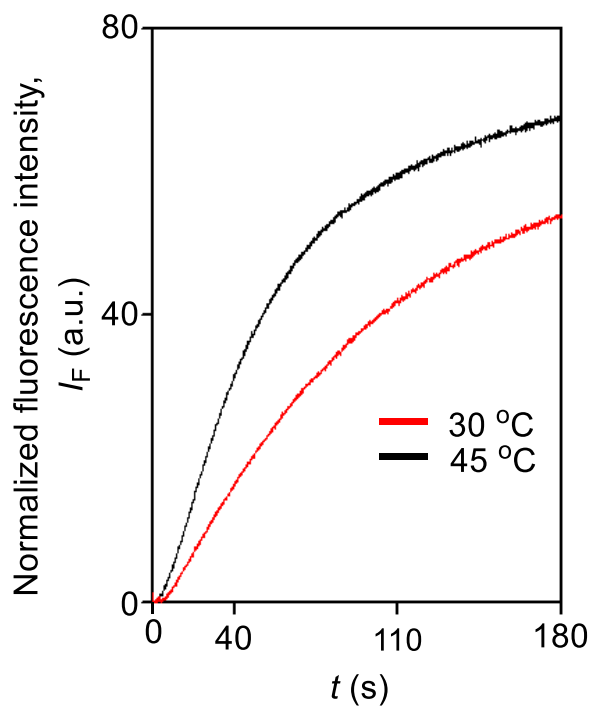


Fig. S10 Ion transport rate of **1d** (1.5 μM) at 30 $^{\circ}\text{C}$ and 45 $^{\circ}\text{C}$ in DPPC-LUVs \supset HPTS vesicles.

VIII. Single Crystal X-Ray Diffraction Study:

The single crystals of **1c** were grown from mixture of acetonitrile and *n*-decane and allowing slow evaporation of the solvents. Single-crystals data were collected on a Bruker SMART APEX four-circle diffractometer equipped with a CMOS photon 100 detector (Bruker Systems Inc.) and with a Cu $K\alpha$ radiation (1.5418 \AA). The incident X-ray beam was focused and monochromated using Micro focus ($I\mu\text{S}$). Crystal of **1c** was mounted on nylon Cryo loops with Paratone-N oil. Data was collected at 100(2) K. Structure was solved by Intrinsic Phasing module of the direct methods and refined using the SHELXTL 2014 software suite.

A

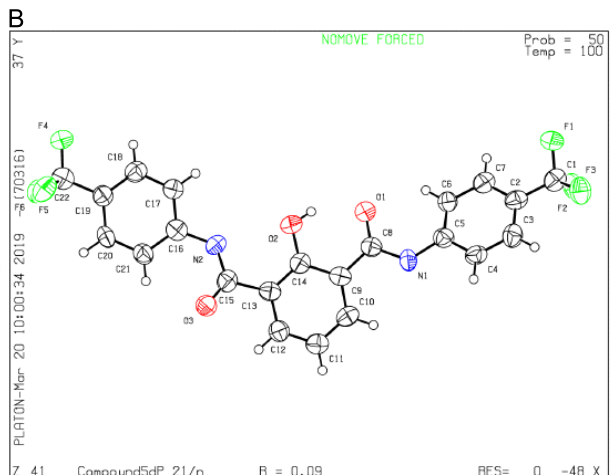
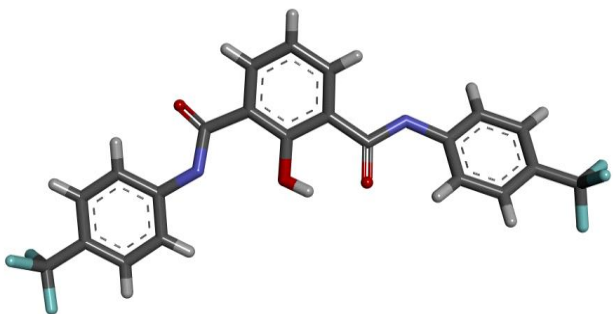


Fig. S11 Single crystal X-ray structure of **5c** (A), and ORTEP diagram of **1c** (B).

Details of the crystal 1c: CCDC 1904396; C₂₂ H₁₂ F₆ N₂ O₃; M = 466.34; Rod shaped; Colorless; Monoclinic; space group P 2₁/n; Cell: a = 10.7749(11), b = 15.2475(15), c = 12.3140(13); Cell volume = 1918.36 Å³, Angles α = 90, β = 108.515(8), γ = 90; GoF = 0.996, Z = 4, T = 100(2), θ_{\max} = 59.85°.

IX. Theoretical Calculations:

To have a clear picture about the channel formation by **1d**, we constructed a theoretical model by predicting the most probable conformation using Conflex 8 program^{S12, 13} (Figure S12). This conformation was used to generate the supramolecular channel model (Figure S13A). Afterwards, the MD simulations were carried out by using an explicit preequilibrated phospholipid bilayer of 128 POPC (1-palmitoyl-2-oleoyl-sn-glycero-3-phosphocholine) molecules obtained from P. Tieleman's University of Calgary website (<http://moose.bio.ucalgary.ca>). The optimized channel was inserted in a box of 128 POPC molecules using inflategro methodology^{S14} at the proper density (area per lipid) of ~ 0.66 nm². To solvate the system, 7544 SPC model^{S15} water molecules were added to the system. GROMOS-53a6 united atom force field^{S16} was used for POPC molecules. The automated topology builder^{S17} created by Malde, *et al.* was used to create the all-atom topology parameters of the channel with GROMOS-53a6 force field. The parameter for potassium ion suitable for GROMOS force field was obtained from the literature.^{S16} The GROMACS 2018.5^{S18} software was used for molecular dynamics to carry out all the simulations.

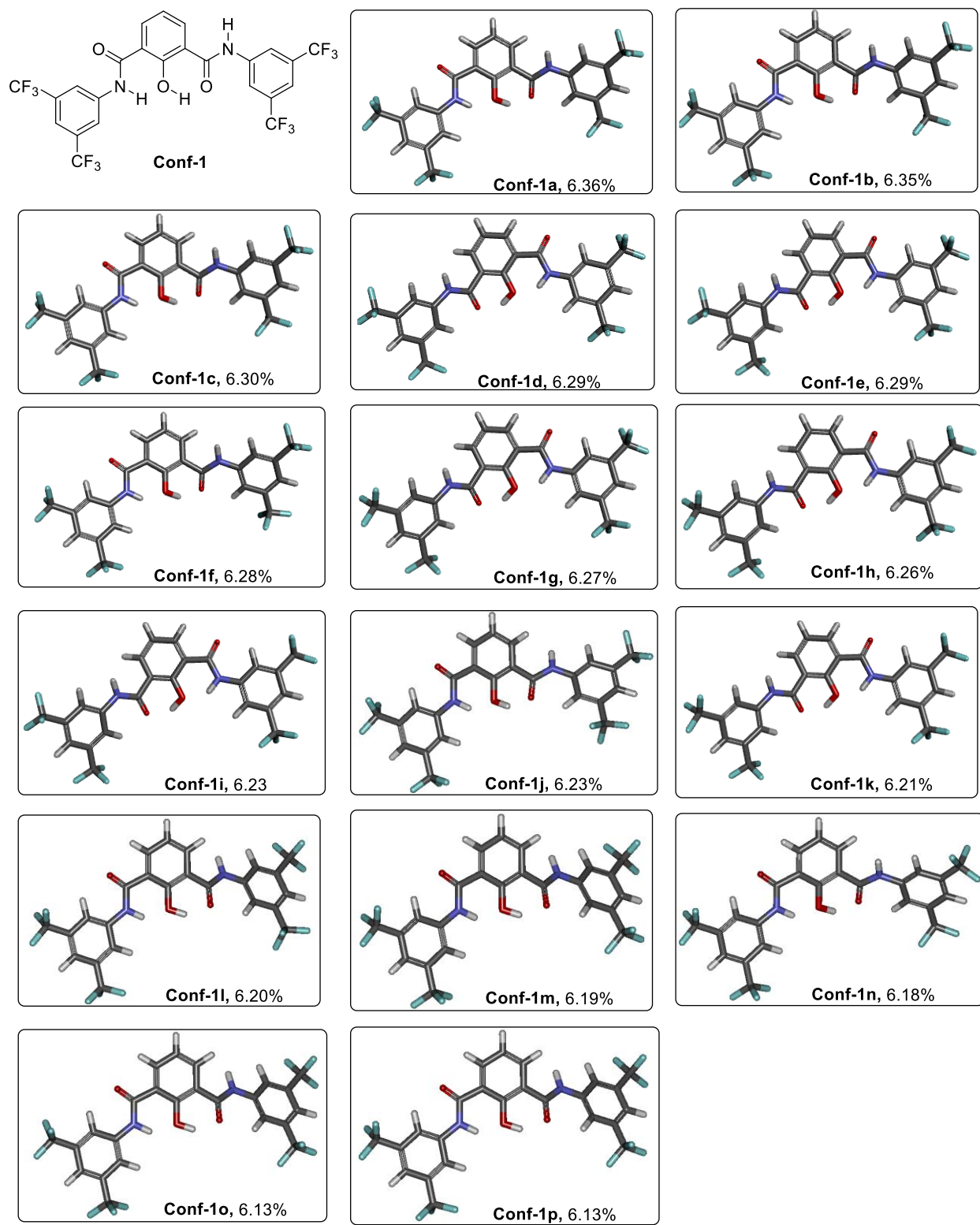


Fig. S12 Geometry optimized structures of two most probable conformations **Conf-1a - Conf-1p** of **1d** along with the Boltzmann distribution of populations.

Initially the system was energy minimized using steepest descent method for 50000 steps. This was followed by equilibration for 1 ns at constant 300 K temperature and 1 bar pressure using Nosé-Hoover^{S19} thermostat and Parrinello-Rahman^{S20} barostat with a coupling constant of 0.5 ps and 2 ps respectively. The equilibrated system is shown in Fig. 5A in the main manuscript. The time step of each simulation was taken as 2 fs. PME^{S21} electrostatics was used for electrostatic interactions using a 12Å cut-off with the van der Waals (vdW) cut-off set at 12 Å. The simulation box was found to be $6.60 \times 6.54 \times 9.23 \text{ nm}^3$ in size after the equilibration step. A final 11 ns molecular dynamics simulation at constant 300 K temperature and 1bar pressure was carried out with similar treatment of temperature, electrostatics and vdW as in equilibration process. The mass density profile across the bilayer was calculated to show how mass is distributed along the membrane axis (set along the Z-direction). The Figure S13B shows the average mass density profiles across the membrane for various lipid components (acyl chain, head groups, glycerol ester and water) and the channel. The density profiles of the lipid components were averaged over the production run of the simulations. The distribution of various lipid components is symmetrical with respect to both of the leaflets in the bilayer. The physical dimensions of the channel were evaluated using HOLE program^{S22} to generate an image of the pore-lining surface and to calculate a pore radius profile of the channel (Figure S13 C) and pore diameter (Figure S13 D).

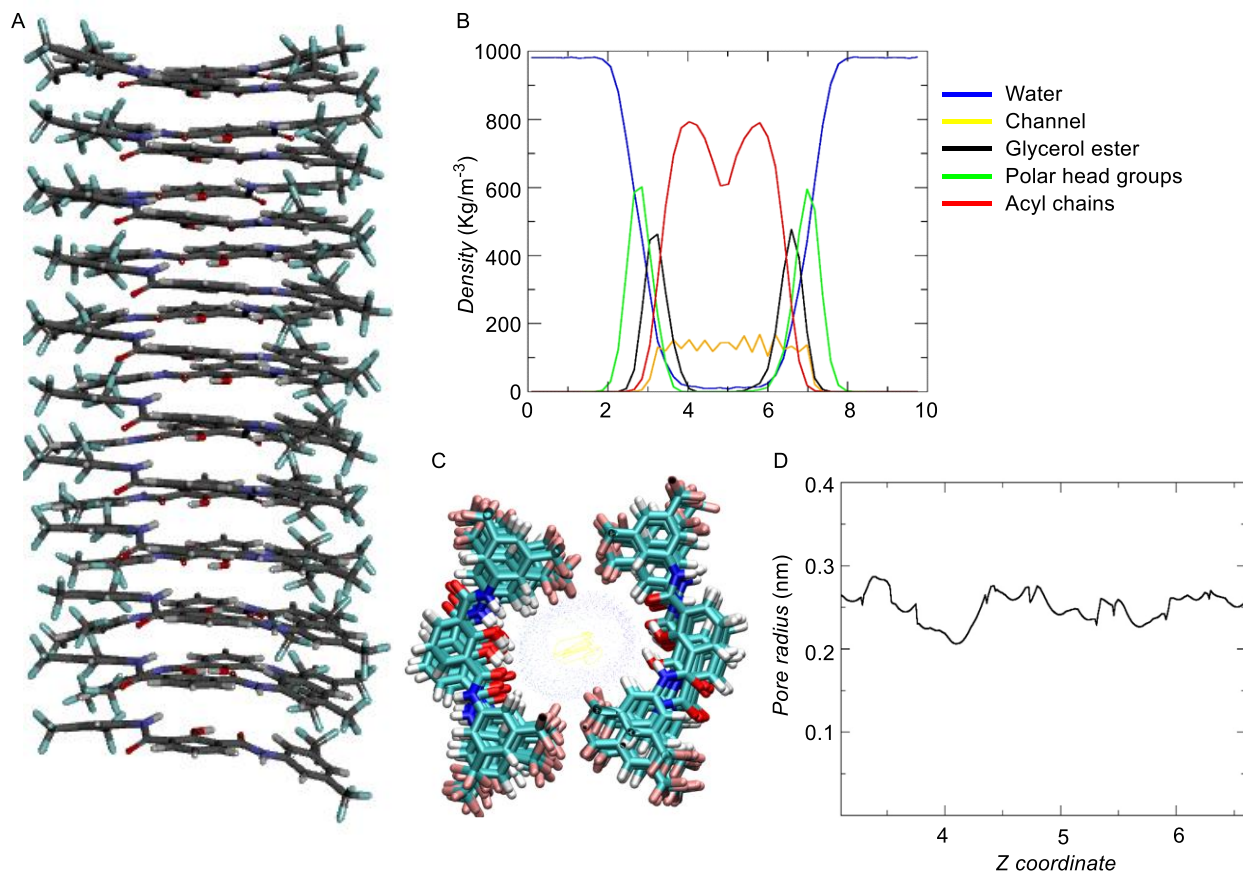


Fig. S13 Side view of the geometry optimized channel formed by **1d** in **Conf-1a** (A), mass density profile of the channel in POPC membrane (B), top view of the pore (C), and variation of pore radius during the simulation (D).

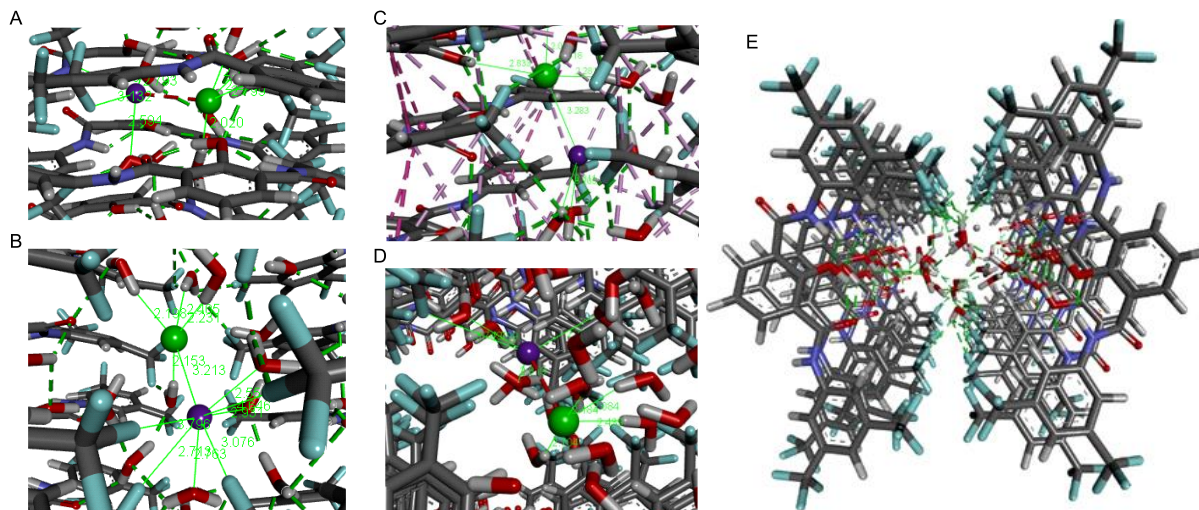


Fig. S14. The zoomed view of snapshots of the frames taken at start (A), at 3ns (B), at 7.5 ns (C), at 10 ns (D), and top view of simulated channel showing hydrogen bonding of C-F and C=O groups of the channel residue.

Noncovalent interactions of the potassium ion: In the simulated system, among the polar functional groups of the individual residues of the channel, the fluorine atoms have shown the maximum interaction energy with the potassium ion rather than carbonyl oxygen, hydroxyl oxygen and amide nitrogen as given in table S2 and Figure S14 A.

Table S2. Average interaction energy between potassium ion and polar atoms of the channel residues.

Atom/s	Total energy (kJ/mol)
Fluorine atoms (red)	-72.5
Amide nitrogen (green)	-5.9
Hydroxyl oxygen (blue)	-9.4
Carbonyl oxygen (black)	-22.0

Noncovalent interactions of the chloride ion: In the simulated system, among the polar functional groups of the individual residues of the channel the phenolic O-H atom has shown the maximum interaction energy with the chloride ion followed by aromatic C-H and amide N-H hydrogen atoms as given in table S3 and Figure S14 B.

Table S3. Average interaction energy between the chloride ion and polar atoms in the channel residues.

Atom/s	Total energy (kJ/mol)
Phenyl hydrogen	-34.9
Hydroxyl hydrogen	-45.5
Amide hydrogen	-19.9

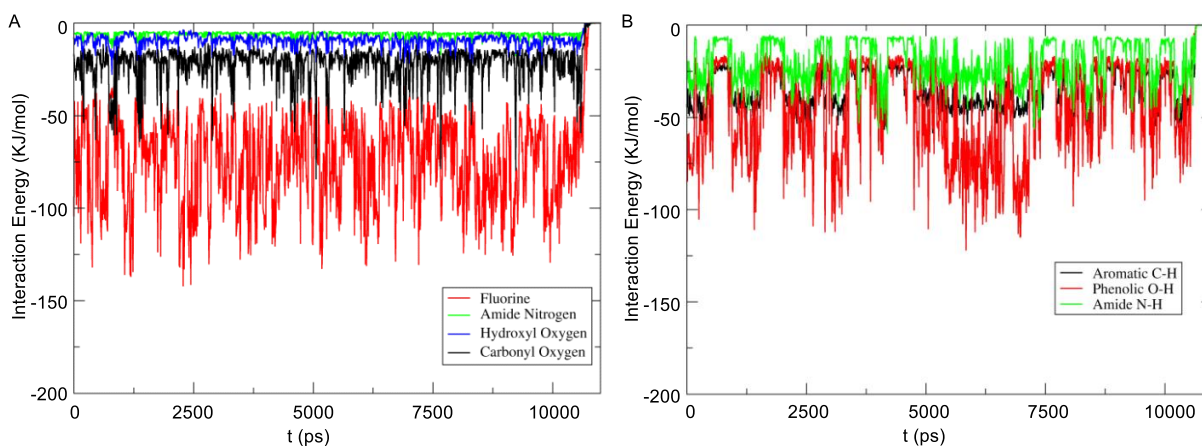


Fig. S15 Energy profile diagram of K^+ (A) and Cl^- ions (B) with different atoms in the channel residues.

Distance between K^+ and Cl^- : The time evolution of the minimum distance between K^+ and Cl^- ion is shown in the figure S13. The distance between the ions was found to be approximately between 0.3 nm to 0.6 nm when the ions were in the channel. When it reaches the bulk water the ions were separated.

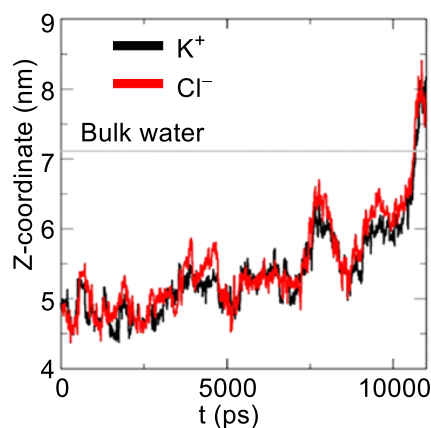


Fig. S16 Positions of ions inside the channel during the simulation.

X. UV-Visible Spectral Studies:

Absorption spectra were recorded on a SHIMADZU, UV-2600, UV-vis spectrophotometer. The absorption spectrum was recorded in commercially available 1X phosphate saline buffer (DPBS) buffer from Lonza. Steady State fluorescence experiments were carried out in a micro fluorescence cuvette (Hellma, path length 1.0 cm) on a Fluoromax 4 instrument (Horiba Jobin Yvon) in Dulbecco's Phosphate-Buffered Saline (DPBS) as well as in lipid phase.

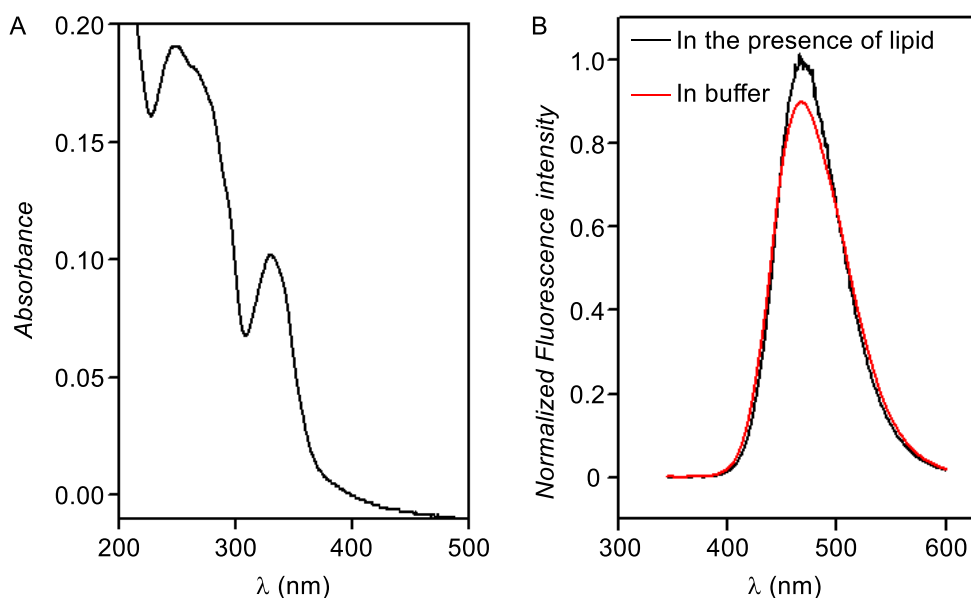


Fig. S17 UV-visible absorbance of **1d** (20 μM) in buffer (A), and normalized fluorescence emission spectra **1d** (20 μM) in buffer and in the presence of lipid (B).

XI. Biological Studies:

A. Cell culture protocol:

The cells were grown in High Glucose Dulbecco's Modified Eagle Medium (DMEM; Invitrogen or Lonza) containing 10% fetal bovine serum (FBS; Invitrogen), 2 mM L-glutamine (Invitrogen) and 100 units/mL penicillin-streptomycin (Invitrogen). Cells were maintained in 100 mm tissue culture treated dishes (Corning) at 37 °C in humidified 5% CO₂ incubator (Thermo Scientific).

B. Live cell imaging:

The MCF 7 cells were seeded in glass bottom 35 mm dishes at the concentration of 5×10^5 cells per plate. After attaining the confluency, the cells were focused in Lieca sp8 confocal microscope and then the DMEM media containing 10 μM of **1d** was added. The blue fluorescent compound was seen in DAPI region using blue LASER. The time course to enter the cell was monitored using real time analysis.

C. MTT-based cytotoxicity assay:^{S15}

Cells were dispersed in a 96-well flat bottom tissue culture treated plates (Corning) at density of 10^4 cells/well (per 100 μ L) and incubated at 37 °C in a 5% CO₂ incubator for 16 h. Compounds were added to each well in different concentration by maintaining maximum amount of DMSO at 2 μ L and incubated for 24 h. DMEM solution containing compounds in each well were replaced with 110 μ L of MTT-DMEM mixture (0.5 mg MTT/mL of DMEM) and incubated for 4 h in identical condition. After 4 h, MTT solution was removed and 100 μ L of DMSO was added in each well to dissolve the formazan crystals. The absorbance was recorded in a microplate reader (Varioskan Flash) at the wavelength of 570 nm. All experiments were performed in triplicates, and the relative cell viability (%) was expressed as a percentage of untreated cells.

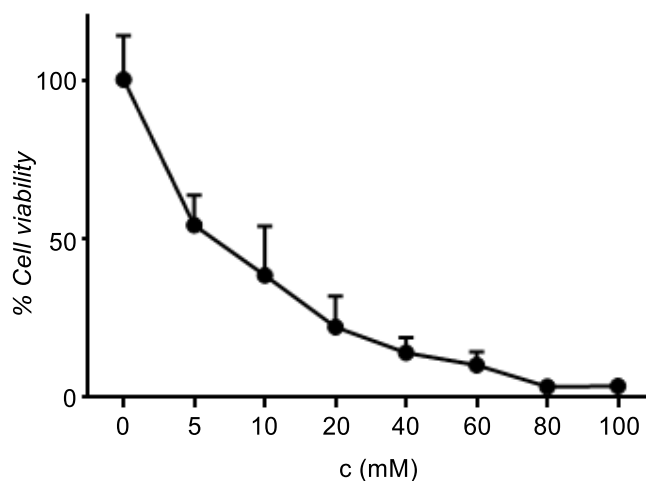


Fig. S18 Cell viability obtained from MTT assay upon **1d** for 24 h in MCF 7 cell lines. Mean cell viability was represented from three independent experiments.

D. Sodium, potassium and chloride mediated cell death studies.

HBSS buffer solution: Hank's balanced salt solution (HBSS with Cl⁻) was prepared with the following compositions: 136.9 mM NaCl, 5.5 mM KCl, 0.34 mM Na₂HPO₄, 0.44 mM KH₂PO₄, 0.81 mM MgSO₄, 1.25 mM CaCl₂, 5.5 mM D-glucose, 4.2 mM NaHCO₃ and 10 mM HEPES (pH 7.4). Chloride free HBSS was prepared by mixing 136.9 mM Na-gluconate, 5.5 mM K-gluconate, 0.34 mM Na₂HPO₄, 0.44 mM KH₂PO₄, 0.81 mM MgSO₄, 1.25 mM Ca-gluconate, 5.5 mM D-glucose, 4.2 mM NaHCO₃ and 10 mM HEPES (pH 7.4). For the Hank's balanced salt

solution without Na⁺ and K⁺, the corresponding salts were replaced with choline salts of the respective ions.

HBSS buffers (all the categories) were mixed with 10% FBS and 1% penicillin-streptomycin before using as extracellular media. Cells were dispersed in a 96-well flat bottom tissue culture treated plates (Corning) at density of 10⁴ cells/well (per 100 μL) and incubated at 37 °C in 5% CO₂ for 24 h. Cellular media was replaced by respective HBSS buffers containing 10% FBS. Compound **1d** was added to each well in different concentration by maintaining maximum amount of DMSO at 1 μL and incubated for 24 h. HBSS buffer solution of compounds in each well was replaced by 100 μL of MTT-DMEM mixture (0.5 mg MTT/mL of HBSS) and incubated for 4 h in identical condition. Excess MTT solution was removed after 4 h and 100 μL of DMSO was added in each well to dissolve the formazan crystals. The absorbance was recorded in a microplate reader (Varioskan Flash) at the wavelength of 570 nm (Figure 10).

E. Mitochondrial membrane depolarization:

The MCF 7 cells were seeded in glass bottom 35 mm dishes at the concentration of 5 × 10⁵ cells per plate. Cells were incubated with 10 μM of **1d** for 24 h. After that cells were washed thoroughly and incubated with JC-1 at the final concentration of 50 nM for 30 min. Fluorescence images were acquired after washing with PBS in both red and green channel using Lieca sp8 confocal microscope. The ratio of pixel intensities (red/green) from 7 different images of each set of cells (by using ImageJ software).

F. ROS generation:^{S16}

The MCF 7 cells were seeded in glass bottom 35 mm dishes at the concentration of 5 × 10⁵ cells per plate. Cells were incubated with 10 μM of **1d** for 24 h. After that cells were washed thoroughly and incubated with DCFDA at the final concentration of 0.5 μM for 20 min. The cell images were acquired after washing with PBS in time dependent manner using green channel with Nikon Eclipse TS 100 fluorescence microscope.

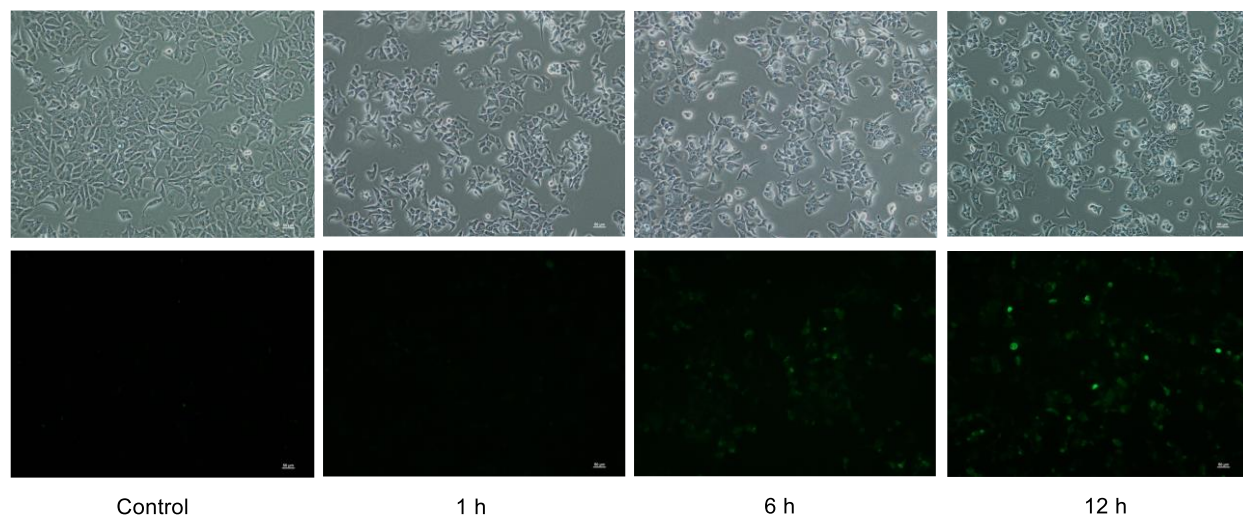


Fig. S19 Live cell images of MCF-7 cells incubated with compound **1d**, and H₂DCFDA as ROS probe (scale bar 50 μ m) in a time dependent manner.

G. Immunofluorescence analysis for cytochrome *c* release:

Cells were seeded at a density of 1×10^5 cells per well on top of glass cover slips (Micro-Aid, India). Following **5d** treatment, cells were fixed using 4% formalin (Macron Chemicals) and were permeabilised using 0.5% Triton X-100 for 10 min at 4 °C. Cells were blocked with 10% (v/v) FBS (Invitrogen), stained with primary antibody (cytochrome *c* antibody) and then incubated with secondary antibody (goat anti-rabbit AlexaFluor-488). Cells were then counterstained with phallogen to stain the cell boundaries and mounted on glass slides (Micro-Aid, India). Cell images were taken in were taken using Leica sp8 confocal microscope. Microscopy images were captured using 63 X oil-immersion objective.

H. Immunoblot analysis:

MCF-7 cells were seeded at a density of 6×10^5 cells per well in 6-well tissue culture treated plates (Corning) and maintained at 37 °C for 24 h. Cells were then treated with 10 μ M of **1d** by direct addition of drug to the culture medium for 24 h at different concentration (10 μ M). Control cells were treated with equivalent volume of DMSO. After 24 h treatment, medium containing **1d** was aspirated and cells were washed once with 1X phosphate buffered saline (PBS; PAN-Biotech GmbH). Cells were lysed in sample buffer containing 60 mM Tris (pH 6.8), 6% glycerol, 2% sodium dodecyl sulfate (SDS), 0.1 M dithiothreitol (DTT) and 0.006% bromophenol blue and lysates were stored at - 40 °C.

Cell lysates were resolved using sodium dodecyl sulfate polyacrylamide gel electrophoresis (SDS-PAGE) and transferred to Immobilon-P polyvinylidene difluoride (PVDF) membrane (Millipore). Blocking was performed in 5% (w/v) skimmed milk (SACO Foods, USA) prepared in 1X Tris buffered saline containing 0.1% Tween 20 (1X TBS-T) for 1 h at room temperature. Blots were incubated for 16 h at 4 °C temperature in primary antibody solution. Following washes, blots were incubated with peroxidase-conjugated secondary antibody solution prepared in 5% (w/v) skimmed milk in 1X TBS-T for 1 h at room temperature following which blots were developed using Immobilon Western Detection Reagent kit (Millipore) and visualized using ImageQuant LAS 4000 (GE Healthcare).

I. Propidium iodide staining:^{S17}

The MCF 7 cells were seeded in glass bottom 35 mm dishes at the concentration of 5×10^5 cells per plate. Cells were incubated with 10 μ M of **1d** for 24 h. The cell plate was washed thoroughly with Phosphate buffer saline (PBS) 2 to 3 times. Then, propidium iodide dye (10 μ g/mL) was added to the plate in dark and the plate was incubated for 15 minutes at 37 °C in CO₂ incubator. After 15 minutes, plates were removed from incubator, dye was removed and the scaffolds were washed thoroughly with PBS to remove the excess stain. 1 mL of fresh PBS was added to the scaffolds, and then analyzed for cell under confocal fluorescence microscope.

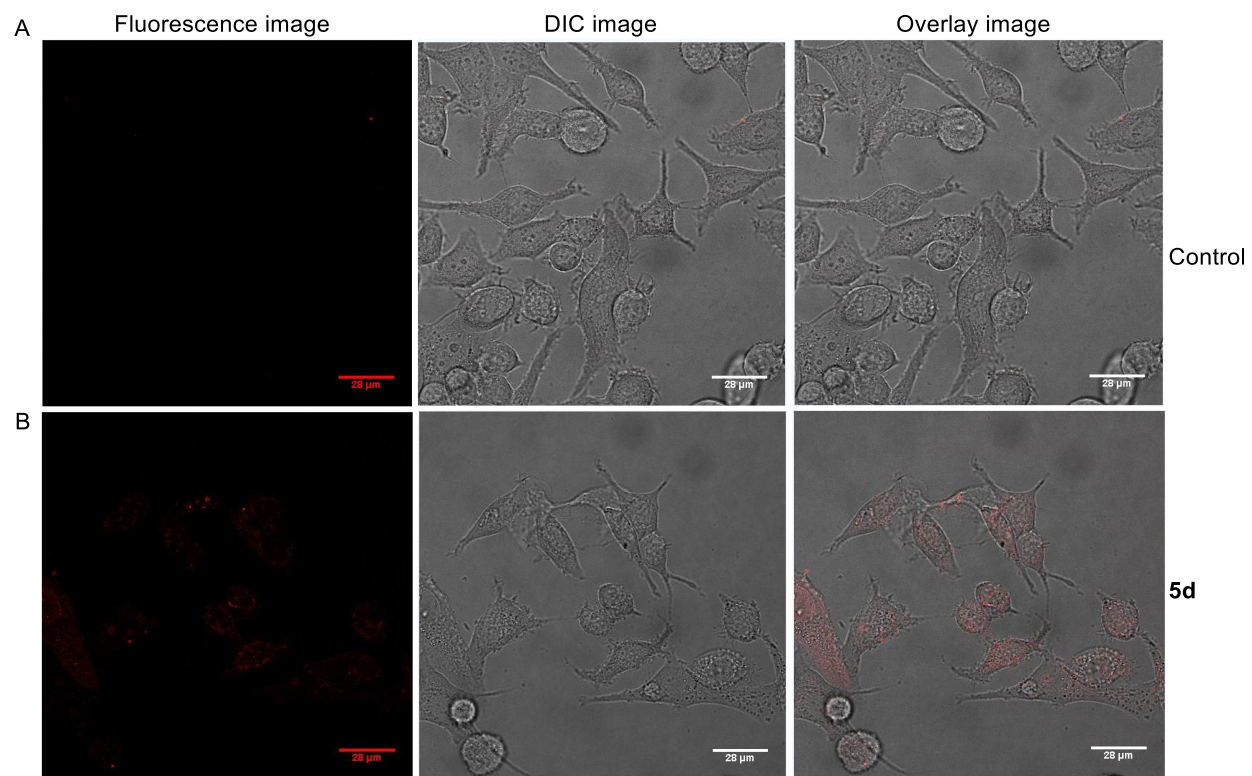


Fig. S20 Live cell images of MCF-7 cells incubated with compound 0 μM (A) and 10 μM of **1d**, and propidium iodide (PI) probe.

XI. NMR Spectra.

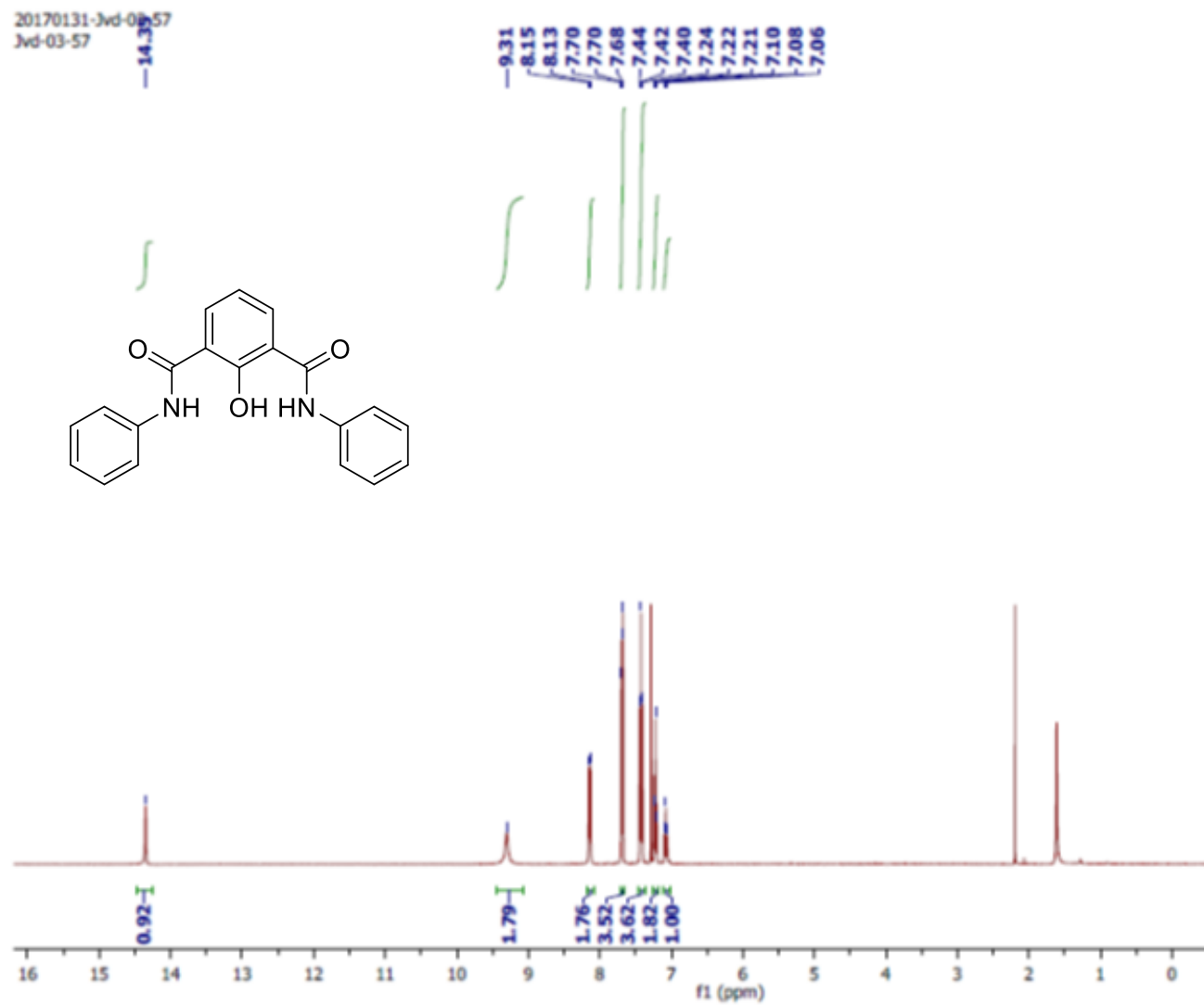


Fig. S21 ^1H NMR spectrum of **1a** in CDCl_3 .

20170207-JVD-03-57
JVD-03-57

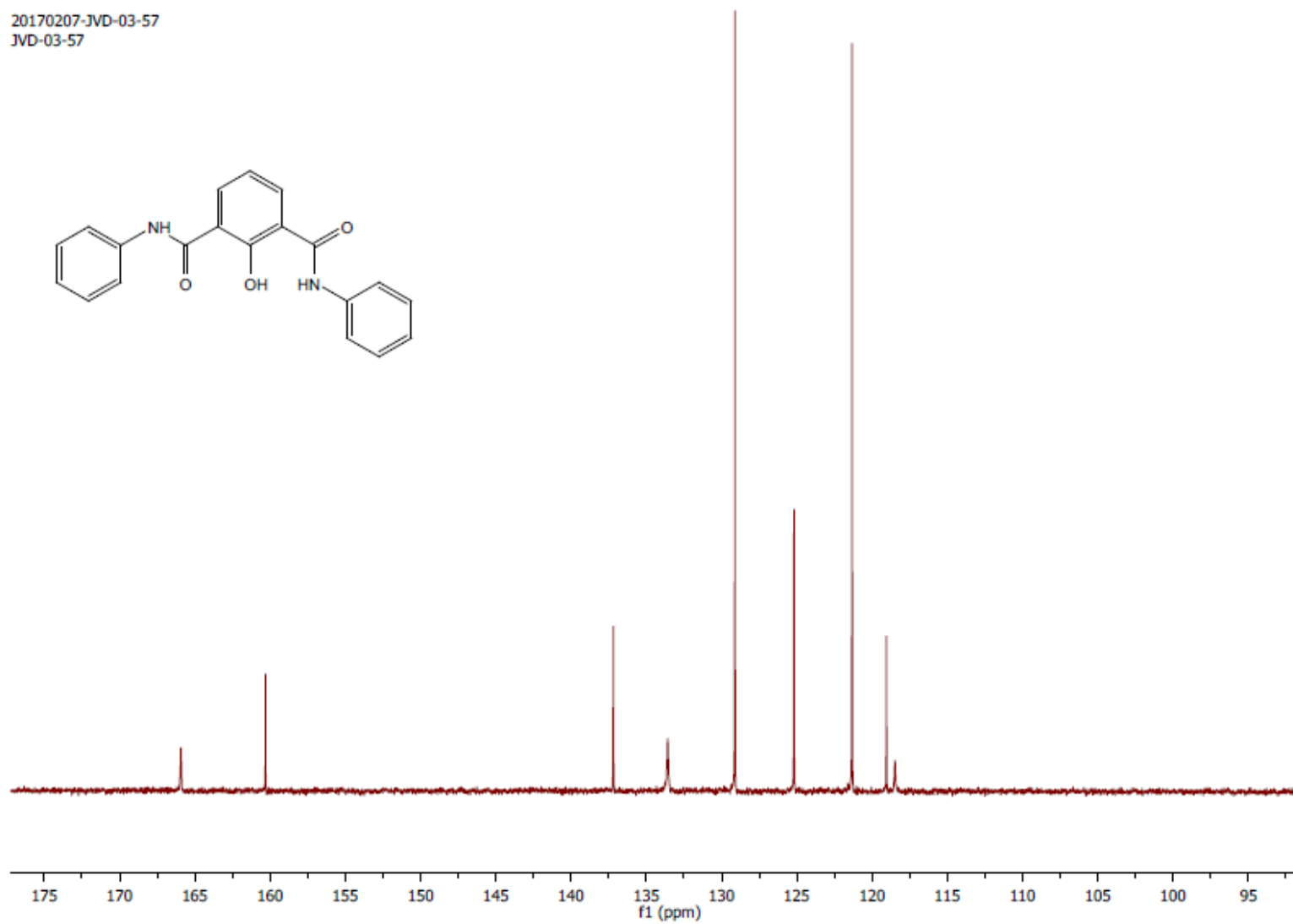


Fig. S22 ^{13}C NMR spectrum of **1a** in CDCl_3 .

20161217-JVD-03-36

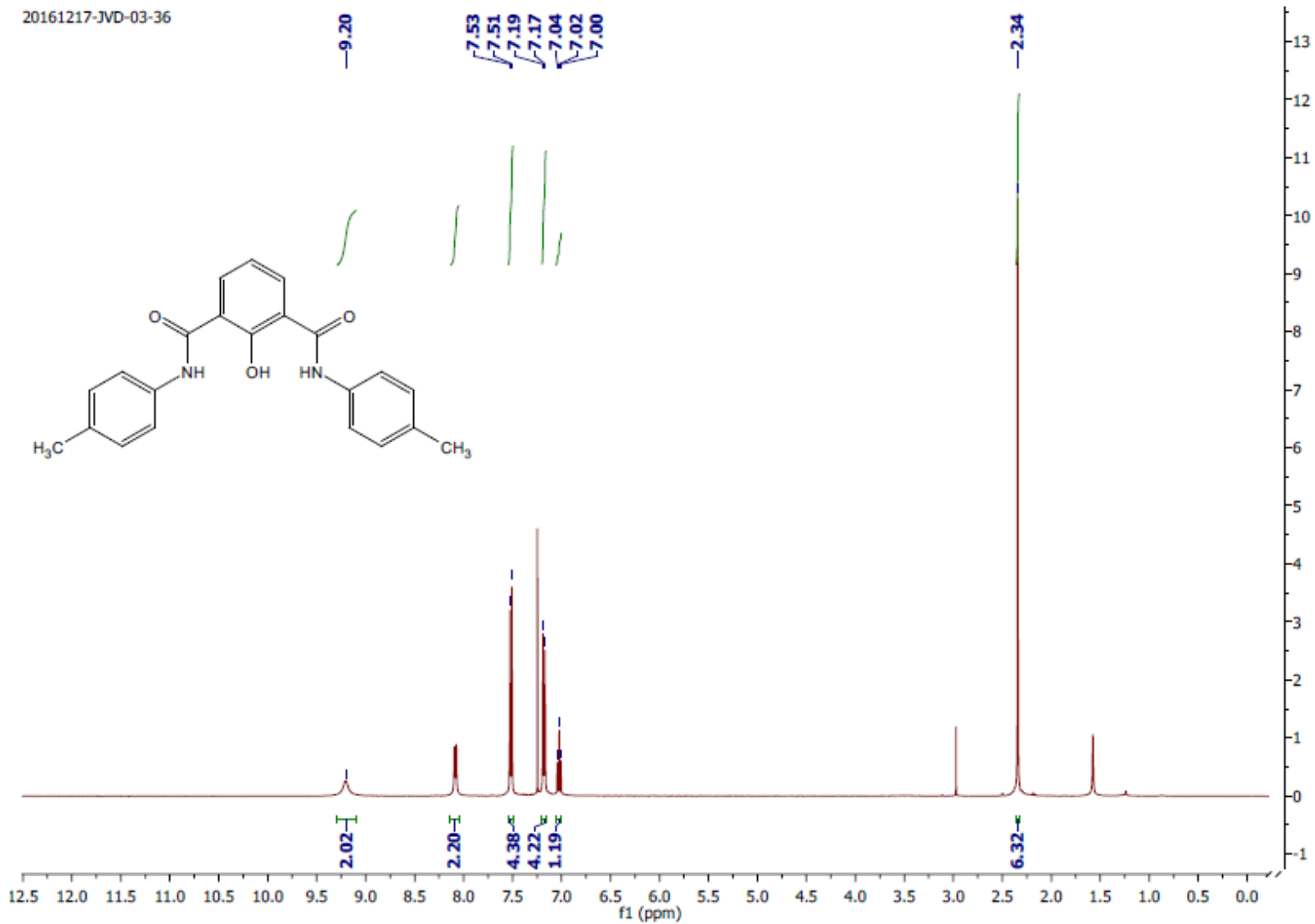


Fig. S23 ¹H NMR spectrum of **1b** in CDCl₃.

20171014-JVD-03-35
JVD-03-35

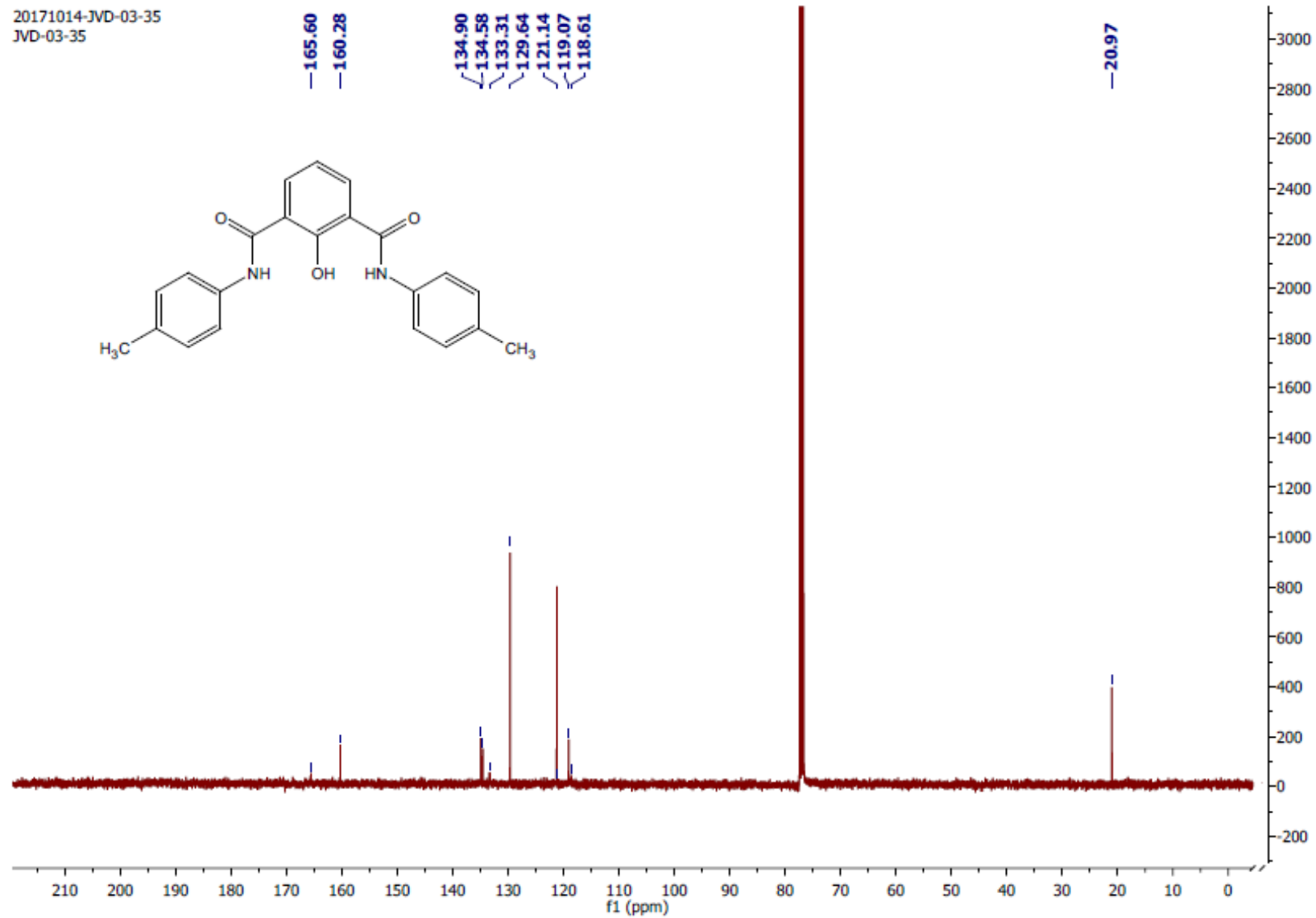


Fig. S24 ¹³C NMR spectrum of **1b** in CDCl₃.

20190309-JVD-025
JVD-025

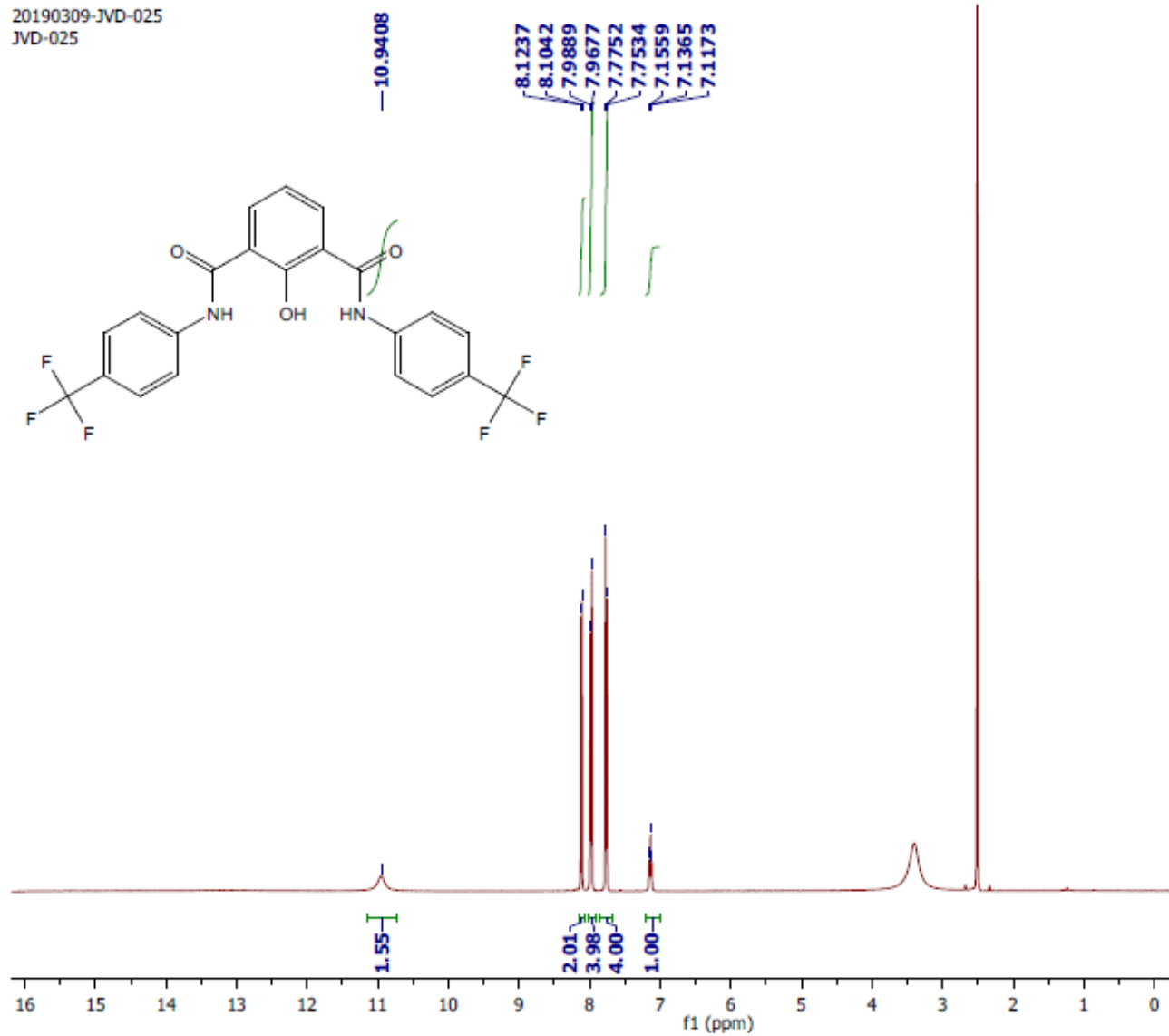


Fig. S25 ¹H NMR spectrum of 1c in DMSO-d₆.

20190309-JVD-025
JVD-025

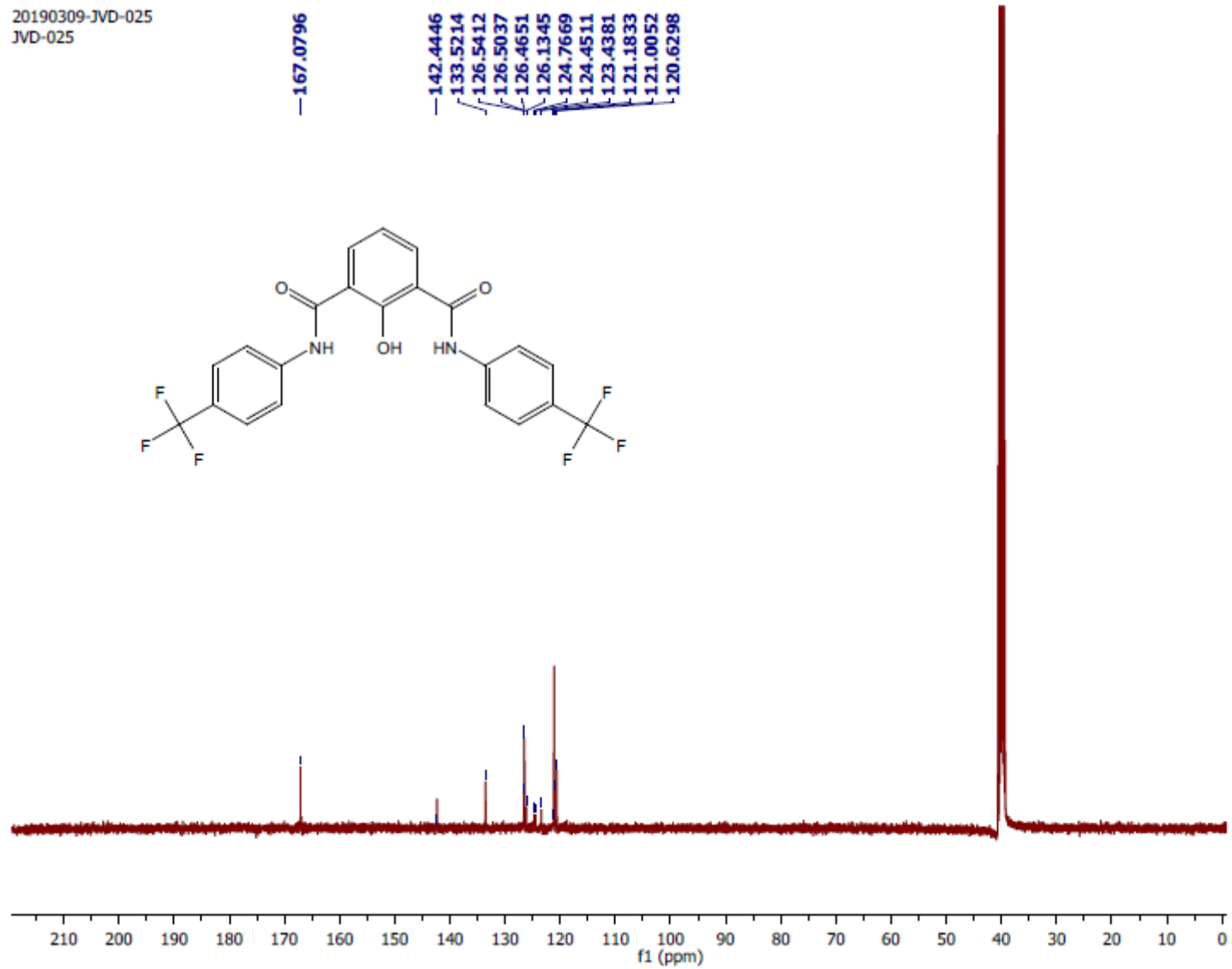


Fig. S26 ¹³C NMR spectrum of **1c** in DMSO-d₆.

20190523-JVD-03-25

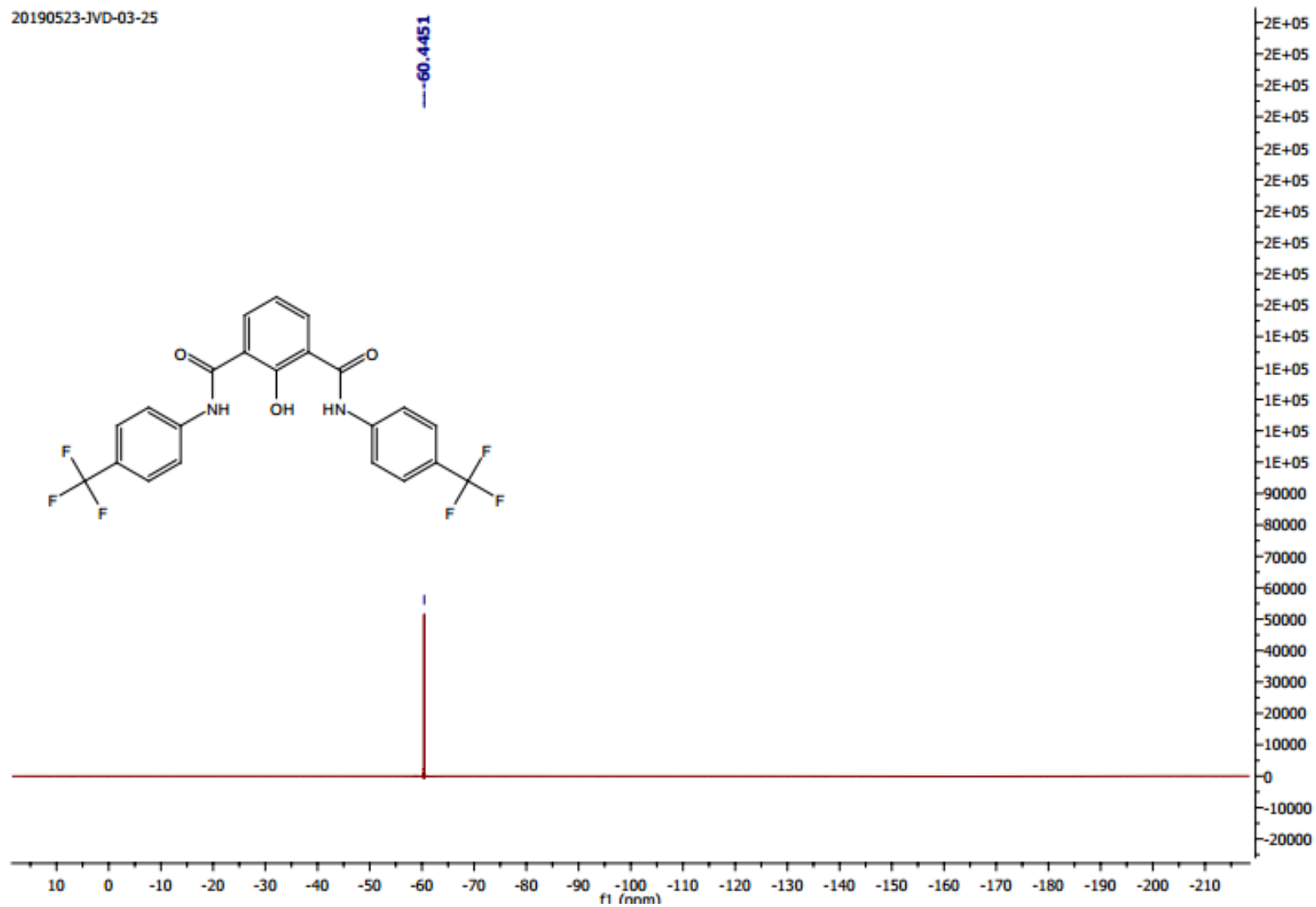


Fig. S27 ^{19}F NMR spectrum of **1c** in DMSO-d_6

20171014-JVD-03-48
JVD-03-48

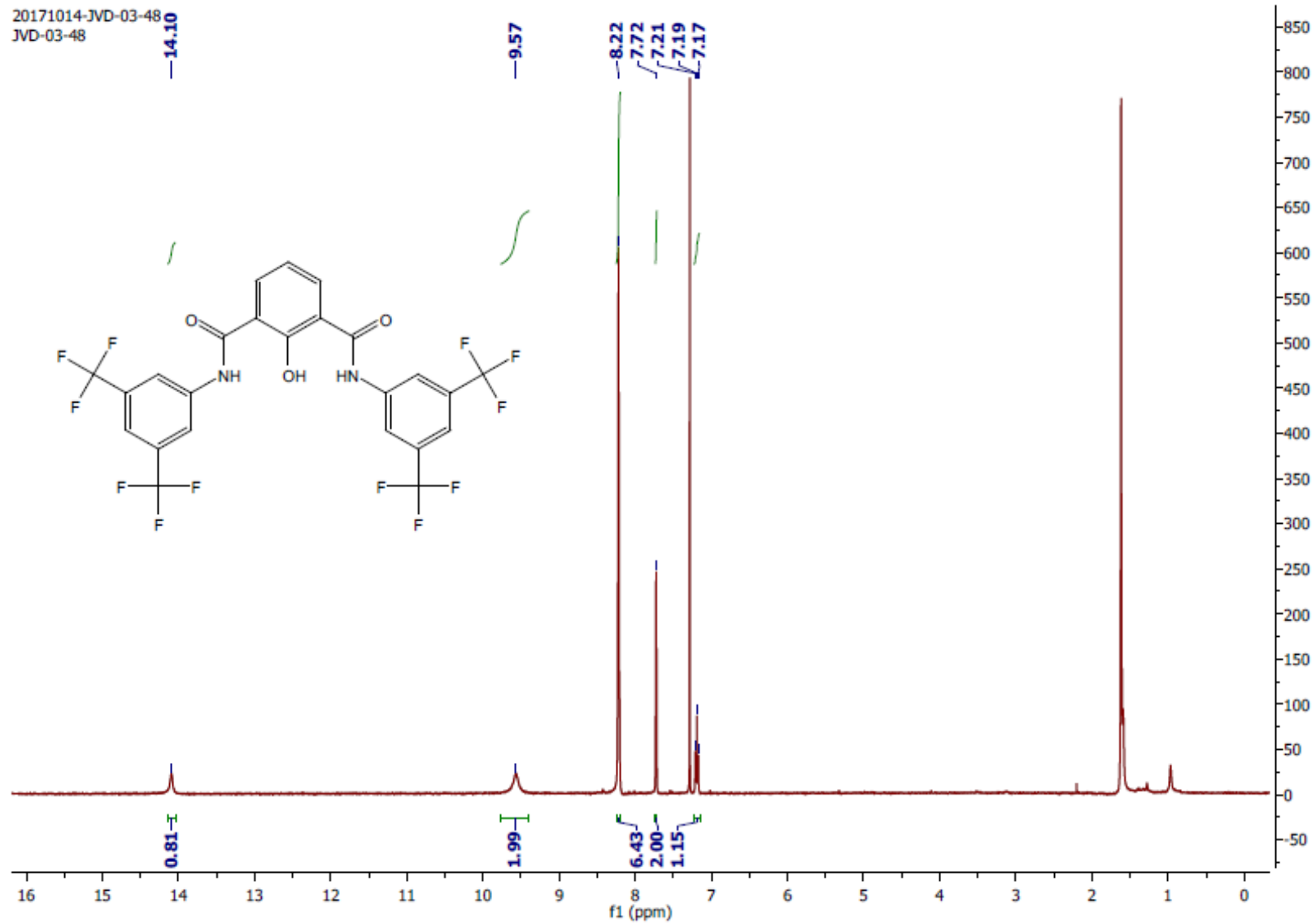


Fig. S28 ¹H NMR spectrum of **1d** in CD₃OD:CDCl₃.

20170207-JVD-03-48
JVD-03-48

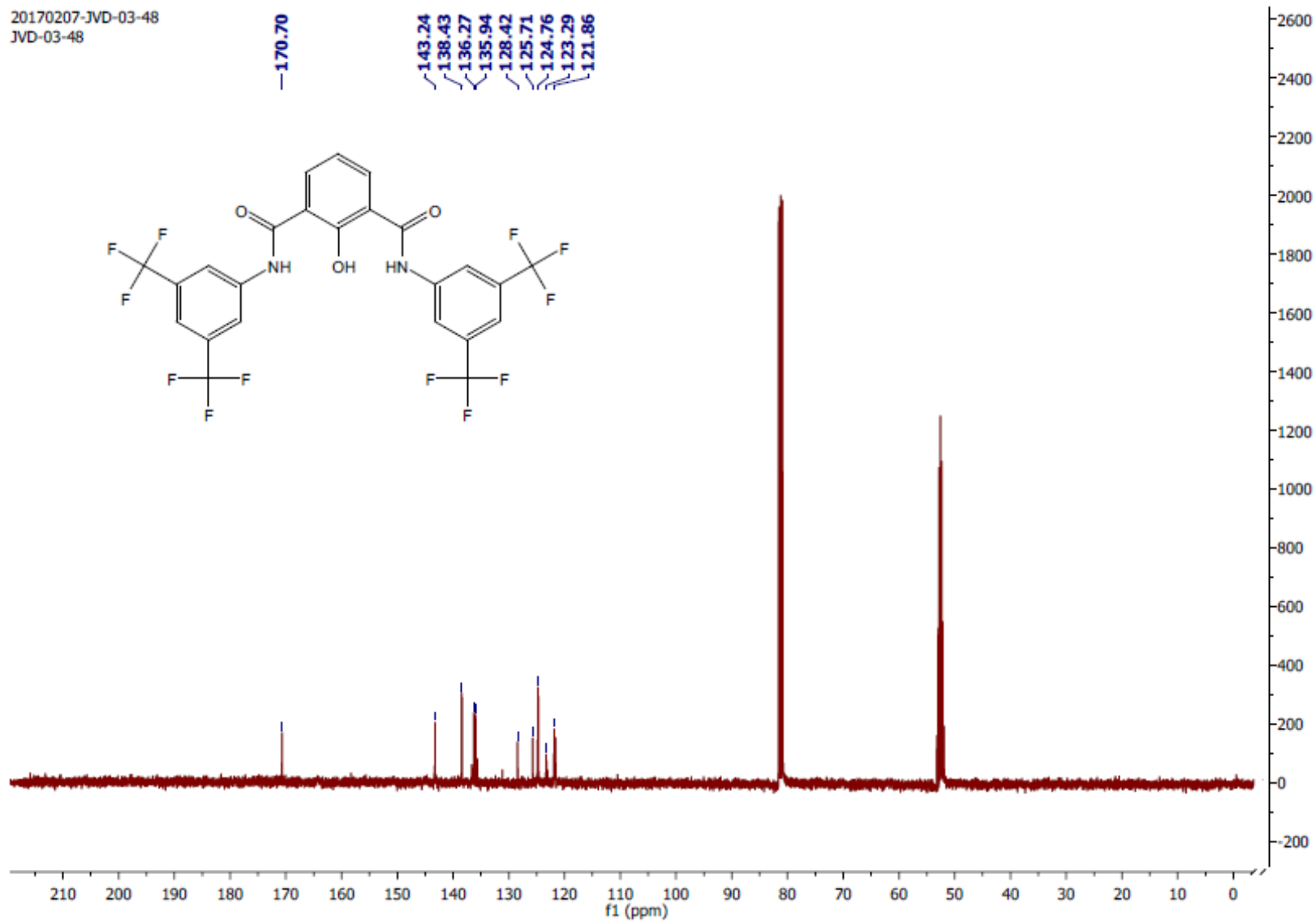


Fig. S29 ¹³C NMR spectrum of **1d** in CD₃OD:CDCl₃.

20190523-JVD-03-48

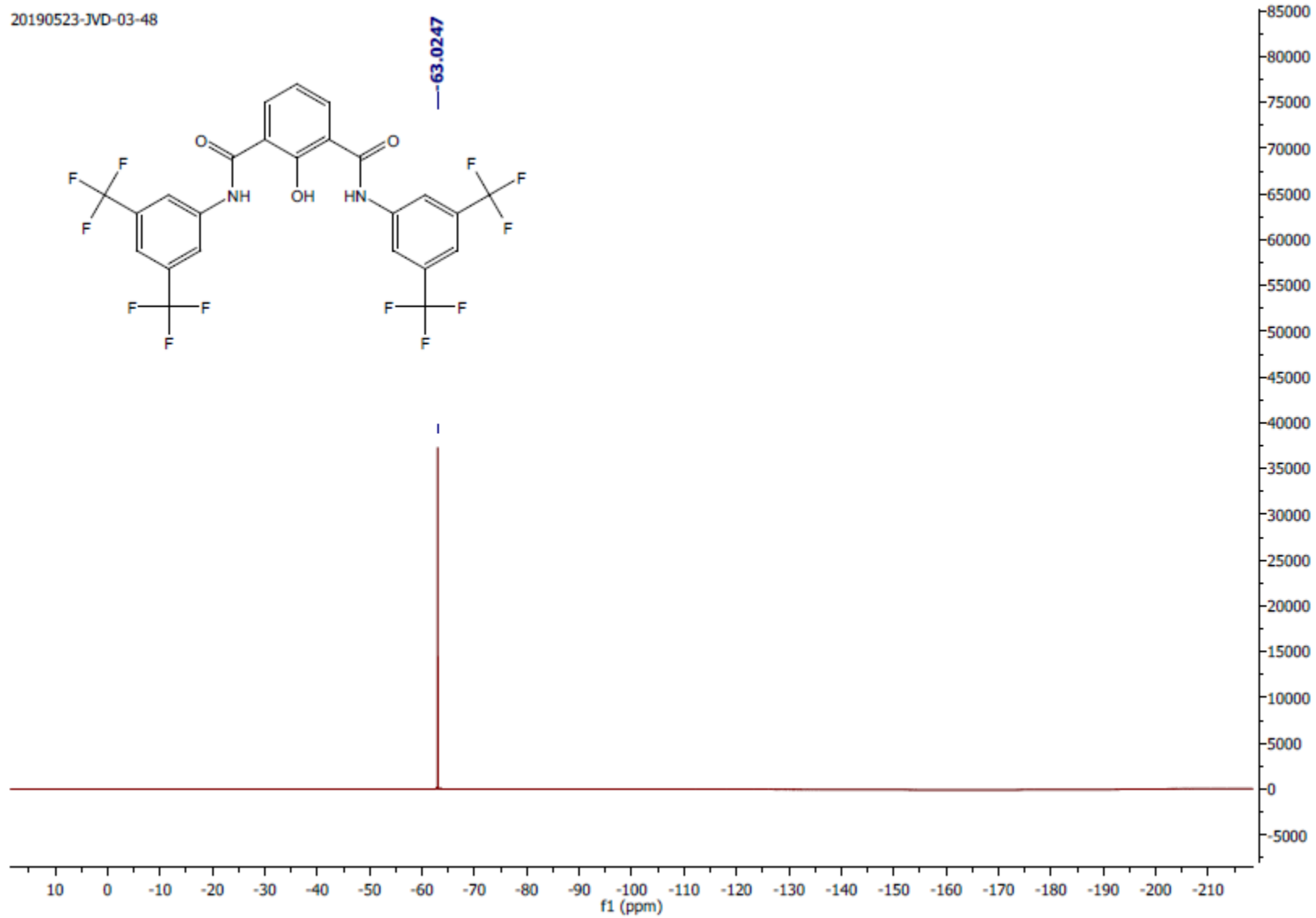


Fig. S30 ^{19}F NMR spectrum of **1d** in $\text{CD}_3\text{OD}:\text{CDCl}_3$.

XII. References:

- S1 Marvin 5.8.0, ChemAxon, 2012 (<http://www.chemaxon.com>).
- S2 A. Kuebel-Pollak, S. Rüttimann, N. Dunn, X. Melich, A. F. Williams and G. Bernardinelli, *Helv. Chim. Acta*, 2006, **89**, 841–853.
- S3 F. Li, V. M. Basile, R. T. Pekarek and M. J. Rose, *ACS Appl. Mater. Interfaces*, 2014, **6**, 20557–20568.
- S4 A. Roy, D. Saha, P. S. Mandal, A. Mukherjee and P. Talukdar, *Chem. Eur. J.*, 2017, **23**, 1241–1247.
- S5 A. Roy, D. Saha, A. Mukherjee and P. Talukdar, *Org. Lett.*, 2016, **18**, 5864–5867.
- S6 J. A. Malla, A. Roy and P. Talukdar, *Org. Lett.*, 2018, **20**, 5991–5994.
- S7 S. V. Shinde and P. Talukdar, *Angew. Chem., Int. Ed.*, 2017, **56**, 4238–4242.
- S8 T. Saha, A. Gautam, A. Mukherjee, M. Lahiri and P. Talukdar, *J. Am. Chem. Soc.*, 2016, **138**, 16443–16451.
- S9 A. Roy, A. Gautam A., J. A. Malla, S. Sarkar, A. Mukherjee and P. Talukdar, *Chem. Commun.*, 2018, **54**, 2024–2027.
- S10 A. V. Jentsch, D. Emery, J. Mareda, S. K. Nayak, P. Metrangolo, G. Resnati, N. Sakai and S. Matile, *Nat. Commun.*, 2012, **3**, 905.
- S11 J. A. Cooper, S. T. G. Street and A. P. Davis, *Angew. Chem., Int. Ed.*, 2014, **53**, 5609–5613.
- S12 H. Goto and E. Osawa, *J. Am. Chem. Soc.*, 1989, **111**, 8950–8951.
- S13 H. Goto, S. Obata, N. Nakayama and K. Ohta, *CONFLEX 8*, CONFLEX Corporation, Tokyo, Japan, 2012.
- S14 T. H. Schmidt, C. Kandt, *J. Chem. Inform. Model.*, 2012, **10**:2657–2669.
- S15 H. J. C. Berendsen, J. P. M. Postma, , W. F. van Gunsteren, J. Hermans, *Pullman, B., Ed.; Reidel: Dordrecht*, 1981, 331–342.
- S16 C. Oostenbrink, A. Villa, A. E. Mark, W. F. van Gunsteren, *J. Comput. Chem.*, 2004, **25**, 1656-1676.
- S17 A. Malde A. et al. (2011) *J. Chem. Theory Comput.*, 2011, **7**, 4026–4037.
- S18 B. Hess, C. Kutzner, D. van der Spoel, E. Lindahl, *J. Chem. Theory Comput.*, 2008, **4**, 435–447.
- S19 S. Nose, *Mol. Phys.*, 1984, **52**, 255–268.

- S20 M. Parrinello, A. Rahman, *J. Appl. Phys.*, 1981, **52**, 7182.
- S21 T. Darden, D. York, L. Pedersen, *J. Chem. Phys.*, 1993, **98**, 10089.
- S22 O. S. Smart, J. G. Neduvelil , X. Wang , B. A. Wallace, M. S. P. Sansom, *J. Mol. Graph.*, 1996, **14**, 354-360.
- S23 T. Saha, M. S. Hossain, D.Saha, M. Lahiri and P. Talukdar, *J. Am. Chem. Soc.*, 2016, **138**, 7558–7567.
- S24 S. Galadari, A. Rahman, S. Pallichankandy and F. Thayyullathil, *Free Radic. Biol. Med.*, 2017, **104**, 144–164.
- S25 T. Suzuki, K. Fujikura, T. Higashiyama and K. Takata, *J. Histochem. Cytochem.*, 1997, **45**, 49–53.